

1 **Constitutive expression of *JASMONATE RESISTANT 1* elevates content of several**
2 **jasmonates and primes *Arabidopsis thaliana* to better withstand drought**

3
4
5 Sakil Mahmud^{1,5}, Chhana Ullah², Annika Kortz³, Sabarna Bhattacharyya¹, Peng Yu^{3,4}, Jonathan
6 Gershenzon² and Ute C. Vothknecht^{1,*†}

7 ¹ Plant Cell Biology, IZMB, University of Bonn, Kirschallee 1, 53115 Bonn, Germany

8 ² Department of Biochemistry, Max Planck Institute for Chemical Ecology, Hans-Knoell-Strasse
9 8, 07745 Jena, Germany

10 ³ Crop Functional Genomics, INRES, University of Bonn, 53113 Bonn, Germany

11 ⁴ Emmy Noether Group Root Functional Biology, INRES, University of Bonn, 53113 Bonn,
12 Germany

13 ⁵ Department of Biochemistry and Molecular Biology, Bangladesh Agricultural University,
14 Mymensingh-2202, Bangladesh

15
16 * Author for correspondence: vothknecht@uni-bonn.de

17 † Senior author

18
19
20 **Short title:** *JAR1* regulates drought stress tolerance

21
22 **One sentence summary:** Constitutive expression of *JAR1* primes *Arabidopsis thaliana* to better
23 withstand drought stress

24
25 ¹Material distribution footnote

26
27 **Key words:** abiotic stress, feedback regulation, growth-defense trade- off, hormone signaling,
28 jasmonic acid, jasmonyl-isoleucine

29
30

¹ The author responsible for distribution of materials integral to the findings presented in this article in accordance with the policy described in the Instructions for Authors (www.plantcell.org) is: Sakil Mahmud (mahmudsakilbau@gmail.com).

31 **ABSTRACT**

32 Jasmonates have a well-documented role in balancing the trade-off between plant growth and
33 defense against biotic stresses. However, the role of jasmonate signaling under abiotic stress is
34 less well studied. Here, we investigated the function of *JASMONATE RESISTANT 1 (JAR1)* in
35 drought stress in *Arabidopsis thaliana*. JAR1 converts jasmonic acid (JA) to jasmonyl-L-
36 isoleucine (JA-Ile), the major bioactive form of jasmonates. Comparison of a newly generated
37 over-expression line (JAR1-OE) with *jar1-11*, a T-DNA insertion line in the *JAR1* locus, and
38 Col-0 revealed that constitutively increased JA-Ile production results in stunted growth and a
39 delay in flowering. Upon water limitation, JAR1-OE plants retained more water in their leaves,
40 showed reduced wilting and recovered better from drought stress than the wild type. By contrast,
41 *jar1-11* mutant plants were hypersensitive to drought. RNA-seq analysis and hormonal profiling
42 of plants under control and drought stress conditions provided insight into the molecular
43 reprogramming caused by the alteration in JA-Ile content. Especially JAR1-OE plants were
44 affected in many adaptive systems related to drought stress, including stomatal density, stomatal
45 aperture or the formation of reactive oxygen species (ROS). Overall, our data suggest that
46 constitutively increased expression of *JAR1* can prime *Arabidopsis* towards improved drought
47 tolerance.

48

49 INTRODUCTION

50 Jasmonic acid (JA) and its multiple derivatives, collectively called jasmonates, are involved in
51 the regulation of plant growth and development as well as biotic and abiotic stress responses
52 (Zander et al., 2020; Wasternack & Hause, 2013; Koo, 2018). JA biosynthesis is initiated by the
53 formation of 13(S)-hydroperoxylinolenic acid (13-HPOT) from plastidal galacto-lipids through
54 different lipoxygenases (13-LOXs), among which LOX2 is the best described enzyme in
55 Arabidopsis leaves (Wasternack & Hause, 2013; Bell et al., 1995). Subsequently, ALLENE
56 OXIDE SYNTHASE (AOS) and ALLENE OXIDE CYCLASES (AOCs) generate 12-oxo-
57 phytodienoic acid (*cis*-OPDA). *cis*-OPDA is immediately transported into the peroxisome and
58 converted into its reduced form by the OPDA REDUCTASE 3 (OPR3). Subsequent steps
59 involving several enzymes of the β -oxidation pathway lead to (+)-7-*iso*-JA. After transport into
60 the cytosol, JA is further modified or conjugated to at least 12 different derivatives, including
61 jasmonoyl-L-isoleucine (JA-Ile), 12- hydroxy-JA-Ile (OH-JA-Ile), 12-hydroxy-JA (OH-JA), 12-
62 *O*-glucoside (12-*O*-Glc-JA), 12-HSO₄-JA and JA-methyl ester (MeJA). All these metabolic
63 products of the jasmonate pathway show varying levels of biological activity (Koo 2018;
64 Wasternack & Hause, 2013).

65 JASMONATE RESISTANT 1 (JAR1), a member of the GH3 family enzymes, holds a key
66 position in jasmonate biosynthesis because it catalyses the formation of JA-Ile from JA
67 (Guranowski et al., 2007; Staswick & Tiryaki, 2004). JA-Ile exerts its function through the
68 formation of a complex with CORONATINE INSENSITIVE 1 (COI1) and various members of
69 the transcriptional repressor JASMONATE ZIM-domain family (JAZ). In the absence of JA-Ile,
70 JAZ together with various co-repressors binds to different transcription factors (TFs).
71 Accumulation of JA-Ile leads to formation of JA-Ile-COI1-JAZ complexes and releases JAZ-
72 mediated suppression of jasmonate responsive genes (Chini et al., 2007; Thines et al., 2007;
73 Katsir et al., 2008; Yan et al., 2009). Jasmonate-dependent TFs can act as activators and
74 repressors and ultimately regulate hundreds of genes. The bHLH protein MYC2 is considered a
75 master regulator of jasmonate signaling (Dombrecht et al., 2007) that affects many JA-Ile
76 mediated responses. Several of the jasmonate-responsive genes, such as vegetative storage
77 proteins (VSP1 and VSP2), have been shown to be regulated by MYC2 (Wasternack & Song,
78 2017; Devoto & Turner, 2005). MYC2 is also a target of gibberellic acid (GA) and abscisic acid

79 (ABA) signaling and thus acts as a central hub for transcriptional regulation of many genes
80 involved in plant growth and defense (Wasternack & Song, 2017).

81 The endogenous JA-Ile concentration is very low, especially compared to other jasmonates (de
82 Ollas et al., 2015b; Balfagón et al 2019). JA-Ile content seems to be tightly controlled via
83 different regulatory loops, including potential auto-regulation of jasmonate synthesis (Hickman
84 et al., 2017). Moreover, the catabolic derivatives of JA and JA-Ile might play a role in
85 maintaining jasmonate homeostasis.

86 Drought is considered one of the major abiotic stresses that negatively affect plant growth and
87 development (Yang et al., 2010). Tolerance mechanisms to drought comprise a wide range of
88 cellular processes including global reprogramming of transcription, post-transcriptional
89 modification of RNA and post-translational modification of proteins, leading to adaptive
90 alteration of metabolism and plant development (Yang et al., 2010). Stress adaptation often relies
91 on the interplay of multiple hormone signaling pathways (Verma et al., 2016) that balance the
92 trade-off between growth and stress protection (Gupta et al., 2020; Yang et al., 2010; Claeys &
93 Inzé, 2013). Drought tolerance mechanisms are closely correlated with ABA signaling, however,
94 interaction with jasmonate signaling occurs both synergistically and antagonistically depending
95 on the plant organ and stimuli (Yang et al., 2019; Daszkowska-Golec & Szarejko, 2013).

96 Exogenous MeJA application can induce drought responsive genes while *vice versa* the exposure
97 to drought induces jasmonate biosynthesis leading to JA-Ile accumulation (Zander et al., 2020;
98 Clauw et al., 2016; de Ollas et al., 2015b; de Ollas et al., 2015a). ROS production is a common
99 reaction to environmental stresses including drought (Noctor et al., 2014). Drought tolerance
100 mechanisms thus include systems to alleviate ROS damage and JA was found to be involved in
101 activating anti-oxidant mechanisms such as regulating the ascorbate-glutathione cycle
102 (Dombrecht et al., 2007; Sasaki-Sekimoto et al., 2005; Xiang & Oliver, 1998; Savchenko et al.,
103 2019). The allocation of metabolic resources to synthesize plant defense compounds is often
104 associated with reduced growth and biomass accumulation. Therefore, plants have evolved
105 various strategies to balance growth and defense trade-offs to maximize their fitness (Guo et al.,
106 2018; Züst & Agrawal, 2017; Claeys & Inzé, 2013; Zhang & Turner, 2008). The role of
107 jasmonates as the prime regulators of such growth-defense trade-offs has been well established
108 in the case of biotic stresses such as herbivory or pathogen infection (Howe et al., 2018; Züst &
109 Agrawal, 2017, Guo et al., 2018; Wasternack, 2017). Whether jasmonates, especially JA-Ile and

110 its derivatives, are also involved in balancing plant growth and drought tolerance remains largely
111 unknown.

112 The first mutant in the *JAR1* locus, *jar1-1*, was identified by its insensitivity to exogenous MeJA
113 application in root growth assays (Staswick et al., 1992). Since then, JA-Ile has been shown to be
114 involved in various plant processes such as pathogen resistance, responses to wounding and
115 insect herbivory, as well as in crosstalk with other hormones (Staswick et al., 1998; de Ollas et
116 al., 2015b; Suza & Staswick, 2008). So far, most work exploring the role of jasmonates in
117 growth regulation and stress response either used external MeJA application or used signaling
118 mutants downstream of JA-Ile synthesis such as *coi1* (Howe et al., 2018; Züst & Agrawal, 2017,
119 Guo et al., 2018; Wasternack, 2017). In this work, we used Arabidopsis lines with altered *JAR1*
120 expression to change the endogenous JA-Ile content and thus explore the role of JA-Ile in plant
121 development and drought tolerance. We could show that alteration in JA-Ile content affects plant
122 growth even under non-stress conditions. While a reduced JA-Ile content in the *jar1-11* mutant
123 makes these plants more susceptible to progressive drought, constitutively increased JA-Ile
124 content in a *JAR1* over-expression line strongly alleviates the deleterious effects of drought,
125 making these plants less sensible and more likely to recover. In depth analysis of RNA-seq data
126 obtained under control and early drought stress conditions provided insight into the
127 transcriptional reprogramming caused by the alteration in JA-Ile content. Based on our results,
128 the potential connection between JAR1-dependent changes in gene expression and differences in
129 Arabidopsis growth and drought response phenotypes are discussed. Overall, our data suggest
130 that constitutive JA-Ile production by increased *JAR1* expression can prime Arabidopsis to cope
131 with drought stress.

132

133

134

135 RESULTS

136 *JAR1* expression levels affect Arabidopsis growth and time of bolting

137 JA-Ile is the central regulator of the jasmonate signaling pathway, and the JAR1 protein holds a
138 key position in jasmonate biosynthesis because it catalyzes the formation of JA-Ile from JA
139 (Guranowski et al., 2007; Staswick & Tiryaki, 2004). To investigate the effect of JA-Ile on plant
140 growth, we used the Arabidopsis TDNA insertion line *jar1-11* (Suza & Staswick, 2008).
141 Moreover, we generated a line expressing YFP-tagged JAR1.1 under control of the 35S promoter
142 (*35S::JAR1.1-YFP*) in the wild type background, which we refer to as JAR1-OE (**Figure 1 and**
143 **Supplemental Figure S1**). Three different splice variants have been predicted for *JAR1* that vary
144 slightly in their exon-intron structure (Zander et al., 2020). Of these, JAR1.1 was the first to be
145 identified (Staswick et al., 2002). In *jar1-11*, insertion of the TDNA into the third exon of the
146 JAR1.1 splice variant was validated at the genomic level by PCR (**Supplemental Figure S1A**
147 **and S1B**). RT-qPCR analysis of rosette leaves under normal growth conditions detected very
148 low expression of *JAR1* transcripts in *jar1-11* (**Figure 1A**), confirming that it is a knock-down
149 but not a null mutant for *JAR1*. By contrast, JAR1-OE plants showed constitutively elevated
150 expression of *JAR1* (**Figure 1A**). Fluorescence microscopy and western blot analysis with a GFP
151 antibody further confirmed the presence of high levels of JAR1.1-YFP protein in rosette leaves
152 of the JAR1-OE line (**Supplemental Figure S1C and S1D**).

153 We first investigated the growth phenotypes of *jar1-11* and JAR1-OE line compared to the
154 respective ecotype Columbia wild type (Col-0). Several studies on jasmonate biosynthetic and
155 signaling mutants had previously shown a moderate insensitivity towards exogenously applied
156 MeJA in root growth assays (Staswick et al., 1992; Xie et al., 1998). When seedlings were grown
157 on ½ MS medium supplemented with sucrose, *jar1-11* plants grew similar as Col-0, while JAR1-
158 OE plants exhibited a retarded root growth phenotype (**Figure 1B; Supplemental Figure S2**).
159 Exogenous MeJA application resulted in a strong reduction of root growth and shoot
160 development in Col-0, while the *jar1-11* plants were much less affected and developed quite
161 well. JAR1-OE plants were most severely affected by MeJA treatment (**Figure 1B;**
162 **Supplemental Figure S2**).

163 Upon extended growth on soil, *jar1-11* plants displayed a slightly larger rosette size than the
164 Col-0, while JAR1-OE plants showed stunted growth with shorter and somewhat wider leaf
165 blades (**Figure 1C and 1D**). Moreover, the number of rosette leaves varied, with the highest in

166 *jar1-11* (~14-16) and the lowest in JAR1-OE (~10-11) (**Figure 1E**). Also, *jar1-11* plants were a
167 few days ahead in bolting and flowering compared to the Col-0, while JAR1-OE plants lagged
168 behind by about 8-10 days (**Figure 1C, 1F and 1G**). Even at the time of bolting, JAR1-OE
169 plants still had fewer and shorter leaves compared to both Col-0 and *jar1-11* (**Figure 1D**). We
170 confirmed our observations using the *jar1-12* mutant, a second TDNA insertion line of the *JAR1*
171 locus, and two additional independent YFP-tagged *JAR1.1* overexpression lines (**Supplemental**
172 **Figure S1A** and **Supplemental Figure S3**). We found similar growth phenotypes, with *jar1-12*,
173 which also had significantly lower *JAR1* transcript levels compared to Col-0 plants
174 (**Supplemental Figure S3A**), growing slightly faster than wild type and showing early
175 flowering, while the JAR1.1 overexpressing lines displaying stunted growth and late flowering
176 (**Supplemental Figure S3B**). All these data indicate that the changes in *JAR1* transcript levels
177 have a strong effect on Arabidopsis growth and development.

178

179 **JAR1 expression levels affect drought tolerance of Arabidopsis**

180 We next used *jar1-11* and JAR1-OE plants to investigate the role of JAR1-mediated JA-Ile
181 formation under drought conditions (**Figure 2** and **Supplemental Figure S4**). We performed
182 progressive drought experiments by withholding water from 18 day-old well-watered plants
183 grown under 16h/8h long-day conditions (**Figure 2A**). After two weeks of water withholding
184 (day 32) at 40% soil water content (SWC), the first indications of drought effects occurred
185 (**Figure 2B** and **Supplemental Figure S4A**). Hypersensitivity of *jar1-11* to drought became
186 clearly visible at 20% SWC (day 36), with plants displaying stronger signs of wilting compared
187 to Col-0. Three days later, at 10% SWC (day 39), both Col-0 and *jar1-11* plants had reached a
188 state of unrecoverable wilting and re-watering at this stage resulted in 0% survival. By contrast,
189 JAR1-OE plants displayed an extended tolerance to drought and showed signs of wilting only at
190 10% SWC (day 39). The mild drought effects seen on the JAR1-OE plants at this time point
191 could be fully reversed by re-watering (**Figure 2B** and **Supplemental Figure S4A**). The
192 drought-susceptible phenotype of *jar1-11* could be confirmed in the *jar1-12* line (**Supplemental**
193 **Figure S4B**). In a separate experiment, the hypersensitivity of *jar1-11* and tolerance of JAR1-
194 OE were also demonstrated by quantifying the leaf relative water content (RWC). At day 36
195 (20% SWC), Col-0 plants retained around 50% RWC, while the RWC of *jar1-11* plants had
196 dropped to about 30%. By contrast, JAR1-OE plants still remained at 80% RWC (**Figure 2C**).

197 We also conducted a similar drought experiment under short-day conditions (**Supplemental**
198 **Figure S5**). Initially, all lines including JAR1-OE were more heavily affected by water loss than
199 under long-day conditions (**Supplemental Figure S5A**). Already after 14 days of water
200 withholding (day 32), the *jar1-11* plants displayed clear signs of wilting. The Col-0 and JAR1-
201 OE plants showed more tolerance, but all three plant lines were heavily wilted by day 39. None
202 of the *jar1-11* plants recovered after re-watering; however, in contrast to the long-day conditions,
203 most of the Col-0 plants (~ 80%) were recovered after one week. Again, all the JAR1-OE plants
204 recovered already after 24 h (**Supplemental Figure S5B**).

205

206

207 **JAR1-dependent changes in jasmonates regulate drought tolerance in Arabidopsis**

208 To further elucidate the role of JAR1 in regulating Arabidopsis drought tolerance, we analyzed
209 the contents of various jasmonates in the different plant lines grown under long-day conditions
210 (**Figure 3**). We collected leaf samples of plants grown under control (well-watered) and drought
211 conditions on day 32 (40% SWC), a time point before severe drought symptoms became visible
212 (**Figure 2B**). Under control conditions, JA-Ile in *jar1-11* plants was virtually absent. By contrast,
213 the JAR1-OE plants accumulated elevated levels of JA-Ile, indicating that substantial amounts of
214 JA-Ile were synthesized and retained in the presence of constitutively elevated JAR1.1 protein
215 (**Figure 3D**). Content of the first committed precursor of jasmonate synthesis, *cis*-OPDA, was
216 slightly increased in JAR1-OE plants compared to Col-0 and the increase was even more
217 pronounced compared to *jar1-11* (**Figure 3G**). On the other hand, content of JA, the direct JAR1
218 substrate, did not change much, with a slight increase observed in *jar1-11* compared to Col-0 and
219 JAR1-OE (**Figure 3A**). With regard to JA derivatives, catabolic products such as OH-JA, OH-
220 JA-Ile and COOH-JA-Ile, showed a substantial increase in the JAR1-OE plants (**Figure 3B, 3E**
221 **and 3F**), suggesting that some of the increased JA-Ile production in these plants led to a greater
222 formation of catabolic products.

223 Drought stress resulted in a significant increase in JA-Ile content in Col-0 and JAR1-OE with a
224 proportionally higher increase in Col-0 even though its JA-Ile content under drought was still
225 much lower than in JAR1-OE under control conditions (**Figure 3D**). By contrast, JA-Ile
226 remained virtually absent in *jar1-11* even under drought stress. However, JA content in *jar1-11*
227 was strongly increased since the pathway to JA-Ile is blocked. (**Figure 3A**). JA levels did also

228 increase in Col-0, but not in the JAR1-OE line, likely because increased JAR1 expression
229 allowed more JA to be converted to JA-Ile and its catabolites. Contents of *cis*-OPDA were
230 reduced in all lines under drought (**Figure 3G**) at levels in line with the formation of JA, JA-Ile
231 and derivatives thereof.

232 *O*-JA-Glc is a less well characterized but highly abundant jasmonates in leaves (Miersch et al.,
233 2008). Its levels were quite similar in all three lines under control conditions and they markedly
234 increased in all lines upon drought stress (**Figure 3C**). Compared to Col-0, the increase was
235 higher in *jar1-11* and lower in JAR1-OE (**Figure 3C**). Similarly, the contents of ABA, which did
236 not differ statistically under control conditions, increased upon exposure to drought stress
237 (**Figure 3H**). Also here the increase was highest in *jar1-11* and lowest in the JAR1-OE plants.
238 Since ABA is the hormone most closely linked to drought stress (Verma et al., 2016), these
239 results suggest that the JAR1-OE line was least affected by drought.

240

241

242 **JAR1-mediated JA-Ile formation regulates many genes involved in Arabidopsis growth** 243 **and drought tolerance**

244 *Transcriptional differences between Col-0, jar1-11 and JAR1-OE under normal growth* 245 *conditions*

246 The strong differences in growth phenotypes of Col-0, *jar1-11* and JAR1-OE plants under
247 normal growth conditions are likely to be controlled by JA-Ile dependent changes in gene
248 expression. To elucidate the global transcriptional changes in these lines, we employed RNA-seq
249 analyses of rosette leaves from 32 day-old well-watered plants grown on soil under long-day
250 conditions (**Figure 4** and **Supplemental Data Set S1**). Using a stringent cut-off (DESeq,
251 adjusted to FDR < 0.01 and LogFC ≥ 1), we found only four differentially expressed genes
252 (DEGs) between *jar1-11* and Col-0 (**Figure 4A; Supplemental Data Set S2**), and all of them
253 were downregulated. By contrast, we found 339 DEGs between JAR1-OE and Col-0 (**Figure**
254 **4A, 4B** and **Supplemental Data Set S2**), of which 134 were downregulated and 205 were
255 upregulated. This is in line with the much stronger phenotypic difference observed between
256 JAR1-OE and Col-0 compared to *jar1-11* and Col-0 at this stage under normal growth conditions
257 (**Figure 1C**).

258 The three genes down-regulated in *jar1-11* (but not JAR1-OE) comprise *JAR1* itself,
259 *ATIG22480* (a potential uclacyanin; cupredoxin superfamily protein) and the well-known
260 jasmonate responsive *VSPI* gene (**Figure 4C; Supplemental Data Set S2**). While the closely
261 related *VSP2* showed only a slight, non-significant decrease in *jar1-11* (**Supplemental Data Set**
262 **S3**), expression of both, *VSPI* and *VSP2*, was upregulated in JAR1-OE plants (**Figure 4C**).
263 Although it is described that JA-Ile accumulation releases transcriptional repression of *MYC2*, a
264 transcription factor and master regulator of JA-mediated signaling (Lorenzo et al., 2004; Kazan
265 & Manners, 2013), we found only a non-significant increase in *MYC2* expression in the JAR1-
266 OE plants under control conditions (**Supplemental Data Set S3**). Expression of *MYC4*, a
267 transcription factor that was suggested to modulate MYC2-mediated regulation (Fernández-
268 Calvo et al 2011; Wasternack & Hause, 2013), however, was significantly decreased in JAR1-
269 OE (**Figure 4C**). In line with the high levels of JA and JA-Ile derivatives, transcripts of *IAA-*
270 *LEUCINE RESISTANT (ILR)-LIKE GENE 6 (ILL6)* and *JASMONATE-INDUCED*
271 *OXYGENASES 3 (JOX3)* were remarkably higher in JAR1-OE. ILL6, a negative regulator of JA
272 signaling, can hydrolyze JA-Ile and 12-OH-JA-Ile to JA and 12-OH-JA, respectively (Bhosale et
273 al., 2013; Widemann et al., 2013). JOX3 is involved in the oxidation of JA to 12-OH-JA
274 (Smirnova et al., 2017). Interestingly, recent studies have shown that 12-OH-JA and 12-OH-JA-
275 Ile both play a role in the modulation of certain JA-Ile regulated processes (Miersch et al., 2008;
276 Jimenez-Aleman et al., 2019; Poudel et al., 2019).

277 In line with the observed differences in development and leaf shape, we found that several of the
278 DEGs upregulated in JAR1-OE as compared to Col-0 are involved in cell cycle control
279 (**Supplemental Data Set S2; Supplemental Data Set S3**), for example, *SYP111 (KNOLLE)*,
280 *FBL17*, *CYCA3;2* and *CYCB1;2* (Gutierrez, 2009). Other genes upregulated in JAR1-OE have
281 functions in cell plate formation (*SYP111* and *CSLD5*), cell wall expansion (*EXPA3*) and cell
282 wall modification (*LTP2*) (Gu et al., 2016; Bernal et al., 2007; Armezzani et al., 2018; Chae et
283 al., 2010). Although *jar1-11* plants showed early and JAR1-OE plants delayed flowering
284 compared to Col-0 (**Figure 1C**), we found no variation in major photoperiod related floral
285 responsive genes such as *FT*, *LEAFY* or *APETALA2* (Zhai et al., 2015). This might be due to the
286 fact that we analyzed leaf samples. However, some of the genes described as part of the
287 autonomous flowering-time pathway have been shown to be expressed in leaves (Mouradov et
288 al., 2002; Cho et al., 2017) and a heat map using a less stringent cut-off of FDR <0.05 and

289 LogFC ≥ 0.5 shows enhancement of *FLOWERING LOCUS C* (*FLC*) expression in JAR1-OE
290 (**Figure 4D**). Early flowering inhibition by FLC involves repression of *SOC1* (Michaels &
291 Amasino, 2001), whose expression was decreased in JAR1-OE, as was the expression of the
292 early flowering inducers *MAF1* (Ratcliffe et al., 2001) and *SPL4* (Wu & Poethig, 2006). On the
293 other hand, expression of *MYROSINASE BINDING PROTEIN 2* (*MBP2*; *F-ATMBP*), which is
294 related to flowering regulation through the CO11 receptor (Capella et al., 2001), was enhanced
295 (**Figure 4D**). Interestingly, even under control conditions, JAR1-OE plants showed down-
296 regulation of certain drought- (*RD29A*, *ERD7*, *LEA14* and *GCR2*) and cold-responsive
297 (*COR15B*) genes compared to Col-0 (**Figure 4B**; **Supplemental Data Set S3**). These genes have
298 been shown or predicted to be ABA-induced (Mizuno & Yamashino, 2008; Liu et al., 2007;
299 Gaudet et al., 2011) and their down-regulation in JAR1-OE suggests that JAR1 mediated JA-Ile
300 accumulation in the presence of low amounts of ABA (**Figure 3H**) might result in the
301 suppression of some stress response pathways.

302

303 *Transcriptional differences between Col-0, jar1-11 and JAR1-OE under progressive drought*
304 *conditions*

305 To investigate JAR1-mediated drought tolerance mechanisms, we also conducted RNA-seq
306 analyses using leaf samples of the different Arabidopsis lines exposed to drought stress (**Figure**
307 **5** and **Supplemental Data Set S1**). As for hormone analysis, samples were taken on day 32
308 (40% SWC) before any severe phenotypic effects became visible (**Figure 2B**). In Col-0, we
309 identified 3401 DEGs, of which 2023 were down- and 1378 upregulated between control and
310 drought conditions (**Figure 5A**). By comparison, *jar1-11* plants, which were most heavily
311 affected by drought stress, showed a much higher number (6139 in total; 2616 up- and 3523
312 down-regulated) of DEGs, while the more drought-tolerant JAR1-OE line displayed a lower
313 number (2025 in total; 971 up- and 1054 down-regulated) of DEGs. Our data indicate that
314 despite any outside appearance of apparent drought effects at the time of sampling, drought had
315 already affected all three plant lines resulting in substantial changes in global gene expression.

316 A comparison of the RNA-seq data between the different plant lines under drought conditions
317 revealed 2411 DEGs between wild type and *jar1-11* (**Figure 5B**; **Supplemental Data Set S2**),
318 among which 966 genes showed a higher and 1445 genes a lower expression level in *jar1-11*. On
319 the other hand, out of 998 DEGs found between Col-0 and JAR1-OE, 737 genes showed a higher

320 and 261 genes a lower expression level in JAR1-OE (**Supplemental Data Set S2**). Moreover, we
321 found 391 DEGs counter-regulated between *jar1-11* and JAR1-OE, most of which showed
322 higher expression in JAR1-OE and lower expression in *jar1-11*. Gene ontology (GO) enrichment
323 analysis confirmed the reciprocal trends between *jar1-11* and JAR1-OE for a number of genes
324 (**Supplemental Data Set S4**), including several genes involved in jasmonate synthesis and
325 jasmonate signaling or known to be jasmonate-responsive (**Figure 5C**). Not surprisingly,
326 expression of the JA responsive transcription factor *MYC2* as well as the *MYC2*-dependent JA-
327 responsive genes *VSP1* and *VSP2* was upregulated in Col-0 and JAR1-OE but not in *jar1-11*
328 (**Supplemental Data Set S3**). Expression of *MYC4*, which had been down-regulated in JAR1-
329 OE under control conditions (**Figure 4C**), remained unchanged but was down-regulated in both
330 *jar1-11* and Col-0 (**Supplemental Data Set S3**). In general, differences between Col-0 and *jar1-11*
331 were more pronounced than differences between Col-0 and JAR1-OE, with many jasmonate-
332 related genes showing lower expression in *jar1-11* upon drought (**Figure 5C**). This includes
333 several of the jasmonate biosynthetic genes upstream of *JAR1*, which showed a lower expression
334 in *jar1-11* under drought compared to Col-0, while their expression was similar or higher than
335 Col-0 in JAR1-OE plants (**Figure 5C**). A similar pattern was also observed for the expression of
336 *MYC2*, *VSP1* and *VSP2* as well as for most *JAZ* genes. By contrast, several enzymes involved in
337 the formation of JA and JA-Ile derivatives, including *JASMONIC ACID CARBOXYL*
338 *METHYLTRANSFERASE (JMT)*, *JOX3*, and *ILL6* showed higher expression in JAR1-OE but
339 similar expression in Col-0 and *jar1-11*. Only a few genes showed higher expression in *jar1-11*.
340 These included the *PEROXISOMAL ACYL-COENZYME A OXIDASE 1 (ACX1)* which is
341 involved in both jasmonate biosynthesis and β -oxidation, as well as *PEROXIGENASE 3 (PGX3)*.
342 Also, two *JAZ* genes, *JAZ1* and *JAZ7*, showed a higher expression level in the *jar1-11* mutant
343 (**Figure 5C**).

344 Not surprisingly, genes known to be responsive to drought and ABA signaling were enriched in
345 the upregulated gene sets of all three lines upon drought (**Supplemental Data Set S2 and S3**).
346 Compared to Col-0 and JAR1-OE, *jar1-11* plants showed a stronger upregulation of several
347 genes involved in the ABA signaling pathway (**Figure 5C**), which is in line with the higher
348 accumulation of ABA under drought (**Figure 3H**). These included genes involved in ABA
349 synthesis, such as *NCED5* and *AAO3*, or *ABI2*, a target gene of ABA regulation (**Figure 5C**).

350 However, we also found that the expression of some genes involved in ABA homeostasis (Xu et
351 al., 2013), such as *CYP707A1*, *CYP707A3* and *UGT71B6*, were higher in *jar1-11*.

352 The major genes with decreased expression in *jar1-11* and increased expression in JAR1-OE
353 were related to photosynthesis (**Supplemental Data Set S4**). This included the light-harvesting
354 complex genes *LHCB6*, *LHCB2.4* and *LHCB4.2*, whose expressions were significantly lower in
355 *jar1-11* and higher in JAR1-OE compared to Col-0 (**Supplemental Data Set S2 and Set S3**). On
356 the other hand, the major genes with increased expression in *jar1-11* and decreased expression in
357 JAR1-OE included various groups of genes responding to abiotic stresses and other hormones
358 (**Supplemental Data Set S4**). Compared to Col-0, JAR1-OE showed a lower expression of
359 several drought-responsive genes such as *LEA46*, *LEA18*, *LEA7* and *RAB18*. These genes were
360 upregulated under drought conditions in the Col-0 (**Supplemental Data Set S2 and S3**),
361 supporting the phenotypic evidence that the JAR1-OE plants did experience less severe drought
362 stress after 14 days of water withholding. At the same time, transcripts of drought-responsive
363 genes such as *DREB2A* or *RD20*, the drought and cold-responsive gene *COR47*, putative
364 drought-responsive genes such as *LEA31*, and hypoxia-responsive genes such as *FMO1*,
365 *At2g25735* and *HIGD2* had a higher expression level in *jar1-11* compared to Col-0,
366 underpinning the greater susceptibility of *jar1-11* to drought stress.

367 To further investigate the differential expression in response to drought compared to control
368 conditions, especially between *jar1-11* and JAR1-OE, we applied hierarchical clustering to all
369 DEGs among Col-0, *jar1-11* and JAR1-OE (**Supplemental Data Set S5**). Using the K-means
370 approach, genes were assigned to 5 clusters. The clusters were then visualized with a heat map
371 (**Figure 6**), revealing general patterns of transcriptomic profiles during drought stress compared
372 to control conditions. These clusters can be categorized into two sets, with the first set of clusters
373 (1-4) representing mechanisms to withstand drought stress effects. We found a decreased
374 expression after drought stress in all lines in clusters 1-4, albeit to a lesser extent in JAR1-OE
375 compared to the wild type and especially to *jar1-11*. Many genes in clusters 1 relate to water
376 transport, while cluster 2 and 4 clearly represent the detrimental effect of drought on the
377 photosynthetic machinery. Genes related to growth regulation were affected on several levels
378 from general regulation of growth (cluster 1) to cell wall biosynthesis and remodeling (cluster 3).
379 Cytokinin response was also negatively affected by drought, especially in *jar-11*, supporting a
380 crosstalk between jasmonates and cytokinin under drought stress. Cluster 5 represents drought

381 stress responses and we found upregulation of ABA-dependent and independent genes related to
382 water deprivation (but also genes related to salt stress, hypoxia, heat stress and oxidative stress as
383 well as some jasmonate mediated biotic stresses) in all lines with the highest upregulation in
384 *jar1-11*.

385

386 **JAR1 regulates stomatal aperture and density**

387 Our RNA-seq analysis had revealed that the expression of *TGG1* and *TGG2*, was highly elevated
388 in the JAR1-OE line under normal growth conditions (**Figure 4B** and **Supplemental Data Set**
389 **S3**). These myrosinases were shown to be involved in ABA- and MeJA-induced stomatal closure
390 downstream of ROS production (Rhaman et al., 2020; Islam et al., 2009). Expression of these
391 genes decreased in all three lines under drought. However, the relative transcript levels in JAR1-
392 OE under drought were still much higher than in Col-0 under control conditions. Similarly, some
393 genes that negatively control stomatal density and distribution, such as *TMM*, *EPF1* or *SBT1.2*,
394 were expressed at higher levels in JAR1-OE under normal growth and drought conditions
395 (**Supplemental Data Set S3**). We thus measured stomatal aperture and density of the 6th rosette
396 leaf of 21 days old Col-0, *jar1-11* and JAR1-OE plants grown under control conditions (**Figure**
397 **7**). We found a higher stomatal density in *jar1-11* compared to Col-0 and JAR1-OE (**Figure 7A**),
398 confirming the role of endogenous JA-Ile content on stomata development. Moreover, *jar1-11*
399 plants also displayed a wider stomatal opening (**Figure 7B**). On the other hand, both the stomatal
400 density and aperture diameter were remarkably lower in JAR1-OE compared to *jar1-11* and Col-
401 0 (**Figure 7A and 7B**). Thus, JAR1-mediated JA-Ile accumulation affects both the aperture and
402 density of stomata, which together can affect the transpirational water loss.

403

404 **JAR1-dependent modulation of the ascorbate-glutathione cycle**

405 ROS production is a common reaction to environmental stresses, including drought (Noctor et
406 al., 2014). Flavonoids, such as anthocyanins, have been suggested to scavenge ROS, and
407 anthocyanin biosynthesis is induced by MeJA application (Shan et al., 2009). Accordingly,
408 JAR1-OE plants had a higher anthocyanin level under control conditions compared to Col-0 and
409 *jar1-11* (**Figure 7C**). Anthocyanin levels increased significantly in all three plant lines upon
410 drought, with the highest increase observed in JAR1-OE plants. Moreover, glutathione plays an
411 important role in preventing oxidative stress by scavenging H₂O₂ through the ascorbate-

412 glutathione cycle pathway (**Supplemental Figure S6**). Some genes coding for enzymes involved
413 in glutathione synthesis or the ascorbate-glutathione cycle pathway were shown to be induced by
414 MeJA application (Xiang & Oliver, 1998; Sasaki-Sekimoto et al., 2005; Zander et al., 2020),
415 while on the other hand, the content of GSH affects MeJA induced stomata closure (Akter et al.,
416 2013). In our experiment, very little difference in expression could be observed between Col-0,
417 *jar1-11* and JAR1-OE under non-stress conditions for genes involved in glutathione biosynthesis
418 or the ascorbate-glutathione cycle (**Supplemental Data Set S3**). Under drought conditions, the
419 GSH producing genes *GSH1* and *GSH2* were downregulated in Col-0 and *jar1-11*, while
420 expression of *DHAR1*, the dehydroascorbate reductase that converts GSH to GSSG, was
421 increased in Col-0 and JAR1-OE (**Figure 7D**). By contrast, expression of *ATGR1* and *ATGR2*,
422 glutathione reductases that convert GSSG to GSH, was increased under drought in Col-0 and to
423 an even greater level in *jar1-11*, but no changes were found in JAR1-OE (**Figure 7D**).

424 To elucidate possible JAR1-mediated effects on ROS regulation, we used the genetically
425 encoded *in vivo* H₂O₂ sensor roGFP-Orp1, which indicates the oxidation level by measuring the
426 H₂O₂/H₂O ratio (Nietzel et al., 2019). We then applied methyl viologen (MV), which was shown
427 to lead to oxidative stress and the generation of ROS, including H₂O₂ (Schwarzländer et al 2009).
428 Treatment of leaf tissue from Col-0 plants with 10 mM MV resulted in a strong oxidative shift of
429 the sensor indicative of oxidative stress (**Figure 7E, Col-0, green line**). Application of 1 mM
430 JA, given together with MV, reduced the MV-induced increase in H₂O₂ levels nearly back to
431 control levels, indicated by a lack of sensor oxidation (**Figure 7E, Col-0, magenta and blue**
432 **lines**). Application of JA alone had no effect on H₂O₂ levels (**Figure 7E, Col-0, orange line**).
433 Application of 10 mM MV to leaf tissue from *jar1-11* plants carrying the roGFP-ORP1 sensor,
434 resulted in a similar oxidative shift as in Col-0 (**Figure 7E, *jar1-11*, green line**). However,
435 application of JA together with MV only resulted in a minor decrease of sensor oxidation in *jar1-*
436 *11*, showing that the MV-induced increase in H₂O₂ level was not much alleviated (**Figure 7E,**
437 ***jar1-11*, magenta line**). This indicates that JAR1-mediated transformation of JA to JA-Ile is
438 required to reduce ROS that are induced by MV.

439
440
441

442 **Discussion**

443 In nature, plants are constantly exposed to various biotic and abiotic stresses. To combat those
444 detrimental effects and maximize their fitness, plants try to strike a balance between growth and
445 stress tolerance mechanisms. Studies had shown that a common set of genes are induced by both
446 externally applied MeJA and drought (Zander et al., 2020; Hickman et al., 2017; Huang et al.,
447 2008). However, the effects of endogenous JA-Ile content on plant growth and drought response
448 remain largely unexplored. Our comparison between *jar1-11* and JAR1-OE demonstrates that
449 JA-Ile plays an important role in regulating processes that help Arabidopsis to withstand
450 progressive drought stress effects. Constitutively increased *JAR1* expression in JAR1-OE plants
451 overrides regulatory circuits that normally reduce JA-Ile content and thus protects plants better
452 from the effects of drought most likely as a result of JA-Ile dependent priming. However, this
453 comes at the cost of retarded growth, delayed flowering and prolonged time until seed
454 production. Therefore, although a consistently high rate of jasmonate signaling due to strong
455 *JAR1* expression might be beneficial for the plant under prolonged drought stress conditions, a
456 more regulated signaling cascade might be a more favorable way to cope with periodic mild
457 drought episodes because it will better promote growth when conditions permit.

458

459 **Overexpressing *JAR1.1* induces jasmonate signaling under non-stress condition**

460 In the current work, we used a TDNA insertion mutant in the *JAR1* locus (*jar1-11*) and a novel
461 transgenic line expressing JAR1.1-YFP under the 35S promoter (JAR1-OE) to alter the
462 endogenous JA-Ile content of Arabidopsis. The *jar1-11* mutant showed a strong reduction in
463 *JAR1* transcripts compared to Col-0 (**Figure 1A**), but a basal level of full-length transcripts is
464 retained despite the disruption of the *JAR1* locus within an exon after about 1/3 of the coding
465 region. Some *JAR1* transcript formation had been shown previously for this line under biotic
466 stimuli (Suza and Staswick 2008). Nevertheless, *jar1-11* plants showed a clear reduction in JA-
467 Ile content and nearly null expression of the jasmonate-dependent defense marker *VSP1*. In the
468 JAR1-OE line, strongly increased *JAR1* transcript levels (**Figure 1A**) result in an about 10-fold
469 increase in JA-Ile content (**Figure 3D**), together with upregulation of *MYC2*, *VSP1* and *VSP2*.
470 Thus, these lines are a great resource to study the effects of varying JA-Ile levels on plant growth
471 and stress responses.

472

473 **Constitutive alteration in *JAR1* levels alters plant growth and development.**

474 The differences in *JAR1* transcript and JA-Ile levels in these transgenic lines manifested
475 themselves in opposite phenotypic alterations compared to Col-0. Differences in growth occurred
476 even under non-stress conditions and were generally more pronounced in JAR1-OE compared to
477 *jar1-11*. Reduced JA-Ile content in the *jar1-11* plants led to a slightly larger rosette size. By
478 contrast, overexpression of *JAR1* resulted in shorter and wider leaves, a similar phenotype also
479 achieved by treating Col-0 plants with exogenous MeJA application (**Supplemental Figure**
480 **S4C**). Exogenous MeJA application has been shown to arrest the cell cycle and thus growth of
481 young leaves (Noir et al., 2013; Zhang & Turner, 2008). However, the initial stunted growth
482 observed in JAR1-OE seems to be superseded at a later stage by increased radial growth of older
483 leaves. Accordingly, expression of the cell cycle controlling gene *CYCB1.2*, which was found to
484 be downregulated after exogenous MeJA application in young seedlings (Zhang & Turner,
485 2008), was upregulated in the older leaves of the JAR1-OE plants used for RNA-seq analysis in
486 our experiments. JAR1-OE plants also seem to have higher expression levels of the transcription
487 co-activators *GIF1* and *GRF5_1* (**Supplemental Data Set S3**), which together were shown to
488 regulate the development of leaf size and shape (Kim & Kende, 2004; Lee et al., 2009). Mutants
489 in the *GIF1* locus had narrower leaf blades compared to wild type indicating that GIF1 supports
490 lateral leaf expansion (Horiguchi et al., 2011; Kim & Kende, 2004; Lee et al., 2009). Altered
491 expression of *GIF1* and *GRF5* in JAR1-OE could be due to the decreased expression of *MYC4*,
492 which was shown to bind the promoter of *GIF1* and downregulate its activity (Liu et al., 2020).
493 Plants of the *jar1-11* and JAR1-OE lines also display opposite phenotypes with regard to
494 flowering time, which is typically controlled by endogenous factors as well as environmental
495 signals. In our analysis, this difference was not reflected by changes in the expression of known
496 photoperiodic floral inducing genes, even though it had been shown previously that COI1
497 inhibits *FT* expression (Zhai et al., 2015). However, JA-Ile independent functions of COI1 have
498 been described recently (Ulrich et al., 2021). Instead, the difference in flowering time could be
499 related to vernalization and the autonomous flowering-time pathway, as evidenced by
500 upregulation of the flowering repressor *FLC* and down-regulation of the FLC-repressed
501 transcriptional activator *SOCI* in JAR1-OE (Michaels & Amasino, 2001; Richter et al., 2019).
502

503 **JA-Ile regulates several physiological systems involved in drought adaptation and stress**
504 **response**

505 Clearly, *jar1-11* plants were more susceptible than Col-0 to the progressive drought stress
506 applied in our study, while JAR1-OE plants only displayed a mild drought stress phenotype. A
507 similar drought stress tolerance was achieved by treating Col-0 plants with exogenous MeJA
508 several days before water was withheld (**Supplemental Figure S4C**). The higher tolerance of
509 JAR1-OE thus seems to be based on changes induced by the elevated JA-Ile content before the
510 plants experienced drought stress. We observed that JAR1-OE plants were able to retain a
511 relatively high water content of more than 80 % even after 18 days of water withdrawal (**Figure**
512 **2C**). This could be due to their smaller stomatal aperture and lower stomatal density observed
513 even under control conditions (**Figure 7A and B**). Regulation of stomatal number and aperture
514 diameter are important mechanisms to mitigate water deficiency. Exogenously applied MeJA
515 was shown to regulate stomatal aperture in leaves (Raghavendra & Reddy, 1987; Hossain et al.,
516 2011). The regulation of stomatal aperture, however, is a very complex process. The higher
517 expression of *TGG1* and *TGG2* in JAR1-OE might play a role, since these myrosinases were
518 shown to be involved in ABA- and MeJA-induced stomatal closure downstream of ROS
519 production (Rhaman et al., 2020; Islam et al., 2009). The lower number of stomata in JAR1-OE
520 already under normal growth conditions seem to be due to increased expression of genes that
521 negatively regulate stomata patterning. This is consistent with the finding that exogenous MeJA
522 application can negatively regulate stomatal development in cotyledons (Han et al., 2018).
523 Drought stress results in an accumulation of cytotoxic H₂O₂ and other ROS (Nocter et al., 2014).
524 But ROS are also generated as secondary messengers and are involved in controlling hormone-
525 dependent stress responses (Xia et al., 2015; Kwak et al., 2006). Controlled redox regulation is
526 thus important to remove cytotoxic ROS levels, while sustaining ROS-dependent regulatory
527 circuits. We could show that external addition of JA alleviates MV-induced H₂O₂ production in
528 Col-0 but not in the *jar1-11* mutant. Previously, external MeJA application was reported to
529 induce some genes involved in the ascorbate-glutathione cycle, one of the major mechanisms to
530 adjust cytosolic H₂O₂ levels (Xiang & Oliver, 1998; Sasaki-Sekimoto et al., 2005; Zander et al.,
531 2020). In our study, we observed upregulation of both *DHAR1* and *GRI/GR2* under drought in
532 Col-0 but differential regulation of these genes in *jar1-11* and JAR1-OE (**Figure 7D and**
533 **Supplemental Figure S6**). We did not see any difference in the expression of ascorbate-

534 glutathione pathway genes under non-stress conditions in JAR1-OE, despite the increase in JA-
535 Ile levels. Together, our data suggest that rather than generally inducing ascorbate-glutathione
536 cycle activity, JA-Ile adjusts the flow through the ascorbate-glutathione cycle under drought
537 conditions. Further studies are required to address this phenomenon, but it might play a role in
538 making the JAR1-OE plants better able to deal with increased H₂O₂ levels upon drought.

539

540 **JA-Ile (and other jasmonates) play a role in drought stress priming**

541 Jasmonates, especially JA-Ile, are at the core of JA-dependent stress responses through COI1-
542 JAZ mediated transcriptional regulations. Interestingly, JAR1-OE plants not only showed an
543 overall higher level of JA-Ile under control conditions but the net increase in JA-Ile under
544 drought also exceeds that observed in Col-0 (**Figure 3**). Levels of the direct precursor JA
545 increased in Col-0 upon drought, while they remain the same in JAR1-OE plants. This might
546 indicate that under drought conditions, even the elevated levels of JAR1 proteins in Col-0 are not
547 sufficient to convert all JA into JA-Ile. It is also likely that factors other than just the amount of
548 JAR1 protein affect JA and JA-Ile levels under stress conditions. The basal level of JA-precursor
549 *cis*-OPDA generally is almost 200 times higher compared to JA-Ile (de Ollas et al., 2015a;
550 Balfagón et al., 2019; Figure 3) and under drought conditions, the magnitude of decrease in *cis*-
551 OPDA content is much higher than the increase in JA-Ile. Together, this indicates that JA
552 production from *cis*-OPDA is not the limiting factor for JA-Ile synthesis. However, the decrease
553 in *cis*-OPDA is at a similar magnitude as the combined increase in JA, JA-Ile and their
554 derivatives such as 12-OH-JA, 12-OH-JA-Ile and COOH-JA-Ile, all of which accumulate to a
555 greater extent than JA-Ile itself. 12-OH-JA and 12-OH-JA-Ile were both found to modulate JA-
556 Ile mediated gene expression, including genes involved in jasmonate biosynthesis (Miersch et
557 al., 2008; Jimenez-Aleman et al., 2019; Poudel et al., 2019). They could thus play a role in
558 balancing the jasmonate responses induced by JA-Ile. Their modulation of certain JA-Ile
559 regulated processes seems to be based on the ability to also act as a bioactive ligands for the
560 formation of COI1-JAZ receptor complexes (Poudel et al., 2019; Jimenez-Aleman et al., 2019).
561 Thus, synthesis of JA-Ile together with the interconversion of JA and JA-Ile into various other
562 derivatives might play an important part in stimuli-specific regulation but likely also in
563 jasmonate homeostasis, i.e. by removal of excess JA-Ile in JAR1-OE under non-stress
564 conditions. Especially intriguing in this respect is the high amount of the JA-derivative 12-*O*-JA-

565 Glc that we found in Col-0, which is in contrast to published data from the Wasilewskija ecotype
566 (Miersch et al., 2008) but is supported by recent findings in poplar (Ullah et al., 2019). Under
567 drought stress conditions, its content increased in all lines, albeit to a lesser extent in JAR1-OE
568 and a greater extent in *jar1-11*. 12-O-JA-Glc has been shown to accumulate 24 hours after
569 wounding of tomato leaves and this accumulation was dependent on jasmonate biosynthesis
570 (Miersch et al., 2008). It was suggested that it might be part of the pathway to remove JA-Ile
571 accumulating under stress. While our study only shows the content of jasmonates at a single (and
572 early) time point during the progressive drought stress, the data lead to the speculation of a stress
573 induced continuous flow of JA-Ile synthesis and removal.

574

575 **Crosstalk between jasmonate and ABA signaling**

576 Studies on various plant species have indicated that ABA and JA-signaling have a complex,
577 interwoven relationship with regard to drought-stress priming and response. With regard to
578 *MYC2* expression, it was shown previously that either jasmonate or ABA alone could induce its
579 expression; however, the effect of both hormones together was much stronger (Lorenzo et al.,
580 2004). This would explain the only slight increase of *MYC2* levels in JAR1-OE under control
581 conditions, where ABA levels are not elevated. Liu and co-workers (Liu et al., 2016) proposed a
582 model, in which exposure to drought activates transcription of *MYC2* via both ABA and
583 jasmonate, which in the form of a positive feedback loop leads to further activation of JA
584 synthesis and subsequently further elevated expression of jasmonate-dependent genes. This is in
585 line with our finding that the expression of *MYC2*, as well as some genes involved in JA
586 synthesis, is increased to a greater extent in JAR1-OE and to a lesser extent in *jar1-11* under
587 drought conditions, when ABA levels are increased. Drought-induced ABA accumulation was
588 evident in all three lines, but was enhanced in *jar1-11* and reduced in JAR1-OE compared to
589 Col-0 (**Figure 3H**). Changes in ABA level corresponded to opposite alterations in the expression
590 of genes related to ABA biosynthesis (**Figure 5C**). However, increase in expression of genes
591 related to ABA biosynthesis in *jar-11* was accompanied by upregulation of genes involved in
592 ABA degradation as well as of *ABI2*, a negative regulator of ABA signaling (Merlot et al., 2001),
593 whose downregulation by exogenous MeJA application was recently described (Zander et al.,
594 2020). Jasmonate signaling could thus also be part of a mechanism to reduce excessive amounts

595 of ABA during drought stress conditions to keep the balance between drought protection and
596 growth.

597

598

599 **Materials and methods**

600 **Plant materials and growth conditions**

601 All experiments in this study were performed on *Arabidopsis thaliana* (ecotype Columbia; Col-
602 0) plants or transgenic lines created in the Col-0 background. The T-DNA insertion lines *jar1-11*
603 (SALK_034543) and *jar1-12* (SALK_011510) were obtained from NASC (Nottingham
604 Arabidopsis Stock Centre, UK) and plants homozygous for the T-DNA insertion were identified
605 by PCR screening (a list of all primers used in this study can be found in **Supplemental Table**
606 **S1**). Plants were grown either on ½ Murashige and Skoog medium (MS) medium (Duchefa
607 Biochemie, Netherlands) with 1% sucrose and 0.6% [w/v] phytigel (Sigma-Aldrich, Inc.,
608 Germany) or on standard plant potting soil pretreated with Confidor WG 70 (Bayer Agrar,
609 Germany). Plants grown on ½ MS were stratified for 2 days at 4°C in the dark. If not otherwise
610 stated, plants were cultured in climatized growth chambers (equipped with Philips TLD 18W of
611 alternating 830/840 light color temperature) at 22°C under long-day conditions (16 h light/8 h
612 dark) with 100 μmol photons m⁻² s⁻¹. In some experiments, short-day conditions (8 h light/16 h
613 dark) were applied.

614

615 **Generation of JAR1-YFP overexpression lines**

616 To generate plants expressing JAR1.1 as a fusion protein with YFP under the control of the 35S
617 promoter (35S::JAR1.1-YFP), the entire coding sequence of the *JAR1.1* variant was cloned into
618 the pBIN19 vector (Datla et al., 1992) in frame with the *YFP* sequence using ApaI and NotI
619 restriction sites. The resulting construct (**Supplemental Figure 1C**) was stably transformed into
620 Arabidopsis wild type using the floral dip method. Three independent homozygous T-DNA
621 insertion lines (JAR1-OE) were obtained each in the F3 generation. JAR1-YFP expression was
622 confirmed through confocal microscopy, RT-qPCR, and western blot using an antibody against
623 GFP (see below).

624

625 **Phenotyping and drought stress experiments**

626 For phenotyping under normal and drought stress conditions, seeds were directly planted in
627 potting soil. Five days later, young seedlings were transplanted to fresh pots containing 100 g
628 potting soil (either one or four seedlings per pot). Plants were grown for 18 days with regular
629 watering with identical volumes of tap water. Afterward, plants were either watered normally or
630 were exposed to drought stress conditions by withholding watering for up to 14 days. During the
631 drought-stress treatment, pot weights were measured regularly. The relative water content of soil
632 (SWC) was calculated from the dried pot weight and adjusted between plant lines to ensure a
633 similar drought stress level. SWC was calculated as $\frac{\text{(pot weight at the time of stress)} - \text{(empty pot weight)}}{\text{(initial pot weight)} - \text{(empty pot weight)}} \times 100$. After SWC dropped to 10%,
634 plants were rewatered with equal volumes of tap water and survival rates of plants were
635 calculated 24 h and 7 d later. At least four independent experiments, each with several plants,
636 were conducted for all experiments. The positioning of all pots in the climate chamber was
637 randomized throughout the experiments. Photographs were taken at regular intervals and
638 corresponding whole rosette leaves were collected for biochemical and RNA-seq analyses on day
639 32.
640

641

642 **Stomatal aperture, density and RWC measurements**

643 Stomatal aperture diameters and density were measured from the 6th leaf of 21 day-old plants by
644 collecting the leaf epidermis as described previously (Hossain et al., 2011). Briefly, excised
645 rosette leaves were floated on a medium containing 5 mM KCl, 50 mM CaCl₂, and 10 mM MES-
646 Tris (pH 6.15) for 2 h in the light (80 μmol photons m⁻² s⁻¹). Subsequently, the abaxial side of the
647 excised leaf was softly attached to a glass slide using a medical adhesive (stock no. 7730;
648 Hollister), and then adaxial epidermis and mesophyll tissues were removed carefully with a razor
649 blade to keep the intact lower epidermis on the slide. Pictures were taken immediately using the
650 bright field option of a confocal microscope (SP8 Lightning, Leica, Weimar, Germany) and the
651 aperture length was processed using the integrated LASX software.

652 The relative water content (RWC) of leaves was calculated according to (Barrs & Weatherley,
653 1962). Briefly, the weight of the whole rosette was measured immediately after collection (W)
654 and after floating them on water for 24 h (TW). Finally, the dry weight (DW) was determined by

655 fully desiccating the leaves in an oven at 70⁰C for 72 hours. RWC was then determined as $\left\{ \frac{(W-DW)}{(TW-DW)} \right\} \times 100$.
656

657

658 ***In vivo* redox imaging**

659 An Arabidopsis line carrying the cytosol-targeted roGFP2-Orp1 sensor previously described by
660 Nietzel et al. (2019), was crossed with *jar1-11*, and homozygous plants of the F3 generation
661 were used for imaging. *In vivo* redox imaging was performed on the leaves of 7-9 day-old
662 seedlings as described in (Meyer et al., 2007) using a Leica SP8 lightning and data were
663 processed using the integrated LASX software with the ‘quantify’ mode. In short, roGFP2 was
664 excited at wavelengths 405 and 488 nm and the emission was detected from 505 to 530 nm. The
665 ratiometric image of 405/488 nm was calculated based on a standardization using 50 mM DTT
666 and 10 mM H₂O₂. Seedlings were pre-incubated in the imaging buffer (10 mM MES, 10 mM
667 MgCl₂, 10 mM CaCl₂, 5 mM KCl, pH 5.8). Subsequently, seedlings were transferred into a
668 perfusion chamber (QE-1, Warner instruments) to allow the exchange to different treatment
669 solutions pumped through a peristaltic pump (PPS5, Multi-channel systems) under constant
670 imaging. Pinhole was adjusted to 3. After each run, representative samples were calibrated with
671 10 mM DTT (ratio = 0.12) and 10 mM H₂O₂ (ratio = 3.0).

672

673 **Anthocyanin measurements**

674 Anthocyanin content was measured according to the modified protocol of (Neff & Chory, 1998).
675 Briefly, whole rosette leaves were ground in liquid N₂, 100 mg of the ground tissue were mixed
676 with extraction buffer (methanol with 1% HCl) and the mixture was placed at 4°C in the dark
677 overnight. After the addition of 200 µl H₂O and 500 µl chloroform, the samples were mixed
678 thoroughly and centrifuged at 14,000 g for 5 minutes. After centrifugation, 400 µl of the
679 supernatant was collected in a new tube and re-extracted with 400 µl of 60% Methanol 1% HCl,
680 40%. The absorbance of the solution was taken at 530 nm (anthocyanin) and 657 nm
681 (background) and anthocyanin content was expressed as (A530-A657) per g fresh weight.

682

683 **Western blot analysis**

684 For extraction of total proteins, leaf samples were first ground in liquid N₂. Approximately 100
685 mg finely ground tissues were mixed with 100 µl 4 x SDS-PAGE solubilizing buffer, vortexed

686 and then incubated at 96°C for 10 minutes. After centrifugation for 10 minutes at 14,000 g,
687 proteins in the supernatant were separated on 10 % SDS-PAGE gels and blotted onto
688 nitrocellulose membranes. Western blot analysis was performed by a standard protocol using an
689 antibody against GFP (α -GFP, Roche) and a secondary antibody coupled with alkaline
690 phosphatase (Pierce Goat Anti-Mouse, ThermoFisher Scientific).

691

692 **Phytohormone analysis**

693 Flash-frozen whole rosette leaves of 32 day-old Arabidopsis plants were ground to a fine powder
694 in liquid N₂. Approximately 50 mg of each sample was extracted with 1 ml methanol containing
695 3 μ l of a phytohormone standard mix (30 ng of D₆-JA (HPC Standards GmbH, Cunnorsdorf,
696 Germany), 30 ng of D₆-ABA (Santa Cruz Biotechnology, Dallas, TX, USA), 6 ng D₆-JA-Ile
697 (HPC Standards GmbH) as internal standards. The contents were vortexed vigorously for 4-5
698 seconds, incubated for 2 min at 25°C, and agitated at 1500 rpm in a heating block. The contents
699 were then centrifuged at 13 000 xg at 4°C for 5 min. Approximately 900 μ l of the supernatant
700 was transferred to new 2 ml microcentrifuge tubes. The residual tissues were reextracted using
701 750 μ l 100% methanol without standards. The supernatants (1650 μ l in total) were completely
702 dried under a flow of N₂ at 30°C and redissolved in 300 μ l 100% methanol.

703 Phytohormone analysis was performed on an Agilent 1260 high-performance liquid
704 chromatography (HPLC) system (Agilent Technologies, Santa Clara, CA, USA) attached to an
705 API 5000 tandem mass spectrometer (AB SCIEX, Darmstadt, Germany) as described by (Ullah
706 et al., 2019). The parent ion and corresponding fragments of jasmonates and ABA were analyzed
707 by multiple reaction monitoring as described earlier (Vadassery et al., 2012). The concentrations
708 of ABA and jasmonates were determined as described previously by (Ullah et al., 2019).

709

710 **RNA extraction, cDNA synthesis and RT-qPCR**

711 Total RNA was extracted from the whole rosette leaves of 32 day-old control and drought-
712 stressed plants using the Quick-RNA Miniprep Kit (Zymo-Research, USA). RNA quality and
713 quantity were determined using a Nabi UV/Vis Nano Spectrophotometer (LTF Labortechnik,
714 Germany). For RT-qPCR analysis, cDNA was prepared from 1 μ g of mRNA with RevertAid
715 First Strand cDNA Synthesis Kit (Thermo Scientific, ThermoFischer Scientific). Gene
716 expression was quantified using the Power SYBR Green PCR Master Mix (Applied Biosystems,

717 ThermoFisher Scientific) in 48 well-plates in a StepOne™ Real-Time PCR Thermocycler
718 (Applied Biosystems, ThermoFisher Scientific) and the expression level was normalized to
719 *Actin2* to express as relative quantity ($2^{-\Delta\Delta C_t}$). A standard thermal profile was used with 50°C for
720 2 min, 95°C for 10 min, followed by 40 cycles of 95°C for 15 s and 60°C for 1 min. Amplicon
721 dissociation curves were recorded after cycle 40 by heating from 60 to 95°C with a ramp speed
722 of 0.05°C/s. Primers used for RT-qPCR are listed in Supplemental Table S1.

723

724 **RNA-seq analysis**

725 For RNA-seq, the quality of RNA was checked by determining the RNA integrity number using
726 a Tapestation 4200 (Agilent). The library preparation and sequencing were performed by the
727 NGS Core Facilities at the University of Bonn, Germany. Approximately 200 ng of RNA was
728 used for library construction. Sequencing libraries were prepared using the Lexogen's QuantSeq
729 3'-mRNA-Seq Kit and sequenced on an Illumina HiSeq 2500 V4 platform with a read length of
730 1x50 bases. For each of the samples, three biological replicates were sequenced with an average
731 sequencing depth of 10 million reads.

732 CLC Genomics Workbench (v.12.03, <https://www.qiagenbioinformatics.com/>) was used to
733 process the raw sequencing data. Quality control and trimming were performed on FASTQ files
734 of the samples. Quality trimming was performed based on a quality score limit of 0.05 and a
735 maximum number of two ambiguities. To map the additional JAR1 reads from the JAR1.1-YFP
736 lines, an additional chromosome comprising the YFP sequence was added to the Araport 11
737 (Cheng et al., 2017) genome and the annotation file. The FASTQ samples were then mapped to
738 the modified Araport 11 genome, while only classifying reads as mapped which uniquely
739 matched with $\geq 80\%$ of their length and shared $\geq 90\%$ identity with the reference genome. For
740 the mapping to the gene models reads had to match with $\geq 90\%$ of their length and share $\geq 90\%$
741 similarity with a maximum of one hit allowed. Subsequently, counts for JAR1.1-YFP and JAR1
742 were combined. Further steps were completed using the R programming language (R Core Team
743 2020). To test the quality of the data, samples were clustered in a multidimensional scaling plot
744 (MDS plot) using plotMDS. To assess differential expression of the sequencing data the
745 Bioconductor package edgeR was used (Robinson et al., 2009). First the read counts were
746 normalized by library sizes with the trimmed mean of M-values (TMM) method (Robinson &
747 Oshlack, 2010). Then common and tagwise dispersion was calculated. For pairwise comparisons

748 the exactTest function to calculate the p-value and the log₂-fold-change were used. The resulting
749 p-values were adjusted by using the False Discovery Rate (FDR) method (Benjamini &
750 Hochberg, 1995). K-means clustering was performed using the kmeans function with the
751 algorithm of Hartigan and Wong (1979) (Hartigan & Wong, 1979). The number of clusters for
752 each clustering was estimated using the elbow method (Thorndike, 1953).

753 GO term enrichment analysis was performed with the topGO package (Alexa & Rahnenfuhrer,
754 2020). The athaliana_eg_gene dataset (Cheng et al., 2017) was downloaded from Ensembl Plants
755 (Yates et al., 2020) via the BioMart package (Durinck et al., 2009). For this a weighted fisher test
756 (Fisher, 1925) was run using the weighted01 algorithm ($p \leq 0.001$). The resulting p-values were
757 adjusted by using the BH method (Benjamini & Hochberg, 1995) filtering for an adjusted p-
758 value ≤ 0.01 .

759 Additionally, Transcripts Per Million (TPM) values were calculated based on the read counts.
760 For individual genes, TPM values were compared by performing an ANOVA (Chambers et al.,
761 1992) and a Tukey's HSD test with a confidence interval of 0.95 (Tukey, 1949). Figures and
762 plots were created using VennDiagram, pheatmap, ggpubr, and EnhancedVolcano included in
763 the R package.

764

765 **Statistical analyses**

766 Data were analyzed statistically with analysis of variance (ANOVA) followed by multiple
767 comparisons (Tukey's honest significant difference [HSD] test) in R v.4.0.3 using the ggplot2
768 package. One-way ANOVA was used to all parameters except hormonal data where two-way
769 ANOVA was applied. For additional experiments, two-tailed t-test was used. Number of
770 replicates and error bars are indicated in the figure legends. Bar plots with error bars were
771 generated in Microsoft Excel, v.16.39. Real-time monitoring of the roGFP2-Orp1 sensor was
772 done using the XY-simple linear regression with 95% confidence level in GraphPad
773 Prismsoftware, v.9.0.0. Information on statistical processing for the RNA-seq are specified in the
774 respective Methods section.

775

776 **Accession numbers**

777 A list of accession numbers is provided in Supplemental Data Set S6.

778

779 **Supplemental Data**

780 **Supplemental Data Set S1:** RNA-seq results from leaf tissue of 32 days old plants grown on
781 soil.

782 **Supplemental Data Set S2:** List of DEGs found between control and drought conditions in each
783 line and between Col-0 and *jar1-11* or JAR1-OE under control and drought conditions.

784 **Supplemental Data Set S3:** Selected DEGs sorted by biological processes.

785 **Supplemental Data Set S4:** GO term enrichment analysis

786 **Supplemental Data Set 5:** Hierarchical clustering of DEGs among wild-type, *jar1-11* and
787 JAR1-OE.

788 **Supplemental Data Set S6:** List of Accession No.

789 **Supplemental Table S1:** List of Primers used in this study.

790 **Supplemental Figure S1:** Confirmation of the TDNA insertion into the *JAR1* locus and
791 overexpression of JAR1.1-YFP.

792 **Supplemental Figure S2:** Effect of exogenous MeJA application on root growth.

793 **Supplemental Figure S3:** Phenotype of the *jar1-12* and additional JAR1-OE lines

794 **Supplemental Figure S4:** Drought stress phenotypes under long-day conditions

795 **Supplemental Figure S5:** Drought stress phenotypes under short-day conditions

796 **Supplemental Figure S6:** Proposed regulation of the ascorbate-glutathione cycle by JA-Ile.

797

798

799 **Acknowledgments**

800 We are grateful to Prof. Dr. Frank Hochholdingher, INRES, Crop Functional Genomics,
801 University of Bonn for facilitating the RNA-seq data analysis in his group. We acknowledge the
802 NGS Core Facility, University of Bonn, for providing the RNA-seq service. Finally, we thank
803 Dr. Fatima Chigri for careful proofreading of the manuscript.

804 **Author Contributions**

805 S.M. and U.C.V. designed the research. S.M., C.U., and S.B. performed the research. S.M., C.U.,
806 A.K., P.Y., J.G., and U.C.V. analyzed the data. S.M., and U.C.V. wrote the paper with input
807 from all authors.

808

809

810 **Figure Legends**

811
812 **Figure 1. Alteration in *JAR1* expression affects *Arabidopsis* leaf growth and flowering time.**
813 **(A)** *JAR1* transcript levels, relative to *ACT2*, in Col-0, *jar1-11* and JAR1-OE determined by RT-
814 qPCR using rosette leaves of 25 day-old plants grown on soil. Data were analyzed by one-way
815 ANOVA (**P<0.01) followed by multiple comparison analysis (Tukey's HSD test). Data
816 represent means \pm SE from three biological replicates (n=3).
817 **(B)** Root length of Col-0, *jar1-11* and JAR1-OE plants grown on ½ MS medium with or without
818 50 μ M MeJA (see also Supplemental Figure S2). Data were analyzed by one-way ANOVA
819 (*P<0.05, **P<0.01) followed by multiple comparison analysis (Tukey's HSD test). Data
820 represent means \pm SE from three biological replicates (n =3), each containing > 10 seedlings.
821 **(C)** Growth phenotype of Col-0, *jar1-11* and JAR1-OE plants grown on soil under long-day
822 conditions after 25 days (upper panel) and 32 days (lower panel).
823 **(D)** Detached rosette leaves at the time of inflorescence stem emergence (~ 1 cm length) of
824 plants grown on soil in long-day conditions. Leaves were detached at day 32 (Col-0), 25 (*jar1-*
825 *11*) and day 40 (JAR1-OE).
826 **(E)** Rosette leaf number of the different plants at day 25. Data represent means \pm SE from five
827 biological replicates (n=5), each containing a minimum of five individual plants.
828 **(F)** Percentage of plants with emerged inflorescence stem of at least 1 cm at day 25.
829 **(G)** Average day by which inflorescence stems had emerged. Data represent means from five
830 biological replicates (n=5), each containing a minimum of five individual plants.

831
832 **Figure 2. Increased *JAR1* expression positively affects drought stress tolerance**
833 **(A)** Schematic representation of the progressive drought stress experiment. Watering was
834 stopped on day 18. Plants were watered again at day 39 when soil water content (SWC) of Col-0
835 plants reached 10%.
836 **(B)** Representative photographs showing plant phenotypes throughout the progressive drought
837 stress experiment (see also Supplemental Figure S4A).
838 **(C)** Leaf relative water content (% RWC) of drought-treated plants on day 32 (40% SWC) and
839 day 36 (20% SWC). Data represent means \pm SE from five biological replicates (n=5), each
840 containing five individual plants. Data were analyzed by one-way ANOVA (**P<0.01) followed
841 by multiple comparison analysis (Tukey's HSD test).

842

843 **Figure 3. JAR1-dependent changes in the contents of jasmonates and ABA.**

844 The contents of different jasmonates (**A-G**) and ABA (**H**) were determined in rosette leaves of
845 32-day old plants from wild type (Col-0), *jar1-11* and JAR1-OE grown under control and
846 drought stress conditions. Compounds measured were jasmonic acid (JA), 12-hydroxy-jasmonic
847 acid (12-OH-JA), 12-hydroxyl-jasmonyl-glucoside (12-O-Glc-JA), jasmonyl-isoleucine (JA-Ile),
848 12-hydroxy-jasmonyl-isoleucine (12-OH-JA-Ile), 12-carboxy-jasmonyl-isoleucine (12-COOH-
849 JA-Ile), 12-oxo-phytodienoic acid (*cis*-OPDA), and abscisic acid (ABA). Data represent means \pm
850 SE from six replicates (n=6), each containing pooled extracts from three plants. Data were
851 analyzed by two-way ANOVA (*P<0.05, **P<0.01, ***P<0.001) followed by multiple
852 comparison analysis (Tukey's HSD test).

853

854 **Figure 4. JAR1-dependent changes in gene expression in rosette leaves under normal**
855 **growth conditions.**

856 **(A)** Venn diagram showing DEGs (DESeq, adjusted to FDR < 0.01 and LogFC \geq 1) in *jar1-11*
857 and JAR1-OE compared to Col-0 in 32-day old plants under normal growth conditions. Arrows
858 indicate up- and downregulation. "O" indicates counter-regulated regulated genes.

859 **(B)** Volcano plot showing statistical significance ($\log_{10}P$) versus magnitude of change (LogFC)
860 of DEGs between Col-0 and JAR1-OE. Violet dots indicate genes that fit the DESeq criteria of
861 FDR < 0.01 and LogFC \geq 1 while green and blue dots represent DEGs that fit only LogFC or
862 FDR, respectively.

863 **(C) and (D)** Heat maps of genes involved in JA biosynthesis, catabolism and signaling response
864 **(C)** or flowering responsive genes **(D)**. Expression was compared between Col-0 and *jar1-11* or
865 JAR1-OE. Data were analyzed using a cut-off of FDR <0.05 and LogFC \geq 0.5.

866

867 **Figure 5. JAR1-dependent changes in gene expression in rosette leaves under progressive**
868 **drought.**

869 **(A)** Number of-DEGs (DESeq, adjusted P < 0.01 and LogFC \geq 1) between control and drought
870 conditions in Col-0, *jar1-11* and JAR1-OE. Arrows indicate up- and downregulation.

871 **(B)** Venn diagram of DEGs (DESeq, adjusted $P < 0.01$ and $\text{LogFC} \geq 1$) in *jar1-11* and JAR1-OE
872 compared to Col-0 under drought conditions. Arrows indicate up- and downregulation. “O”
873 indicates counter-regulated genes.

874 **(C)** Heat maps of genes involved in JA biosynthesis, catabolism and signaling response (left) as
875 well as ABA biosynthesis, catabolism and signaling response (right) compared between Col-0
876 and either *jar1-11* or JAR1-OE, all under drought conditions. Data were analyzed using a cut-off
877 of $\text{FDR} < 0.05$ and $\text{LogFC} \geq 0.5$.

878

879 **Figure 6. JAR1-dependent transcriptomic variations between drought stress and control**
880 **conditions.**

881 Heat map (left) and K-means clustering (middle) of genes up- or downregulated under drought
882 stress compared to control conditions in the different plant genotypes. K-means clustering
883 analysis was performed to produce the clusters (DESeq, adjusted $\text{FDR} < 0.01$ and $\text{LogFC} \geq 1$)
884 and the thin lines represent the mean expression profiles for each cluster (middle). Only genes
885 that are differentially expressed in at least one of the comparisons were used for the cluster
886 analysis. The top two GO terms for each cluster with P values are listed (right).

887

888

889 **Figure 7. Effect of JA-Ile on stomatal regulation, anthocyanin content and MV-induced**
890 **changes in redox status.**

891 **(A)** and **(B)** Number of stomata **(A)** and stomatal aperture **(B)** measured on leaf No. 6 of plants
892 grown under control conditions at day 21. Data represent means \pm SE from three biological
893 replicates (n=3). For stomatal numbers, each replicate quantified leaves from 5-6 individual
894 plants. For stomatal aperture, each replicate quantified 90 to 100 stomata in leaves from 6-10
895 individual plants. Data were analyzed by one-way ANOVA (*P<0.05, **P<0.01) followed by
896 multiple comparisons (Tukey's HSD test).

897 **(C)** Anthocyanin content of different plant genotypes determined in rosette leaves of 32-day old
898 plants grown under control and drought stress conditions. Data represent means \pm SE from 3
899 replicates (n=3), each containing three pooled individual plants. Data were analyzed by one-way
900 ANOVA (*P<0.05, **P<0.01) followed by multiple comparisons (Tukey's HSD test).

901 **(D)** Heat maps of DEGs involved in the ascorbate-glutathione cycle in *jar1-11* and JAR1-OE
902 compared to Col-0 under drought conditions (left) or between control and drought conditions in
903 Col-0, *jar1-11* and JAR1-OE (right). Data were analyzed using a cut-off of FDR <0.05 and
904 LogFC \geq 0.5. White boxes indicate genes whose changes did not meet the cut-off criteria.

905 **(E)** Real-time monitoring of redox status using cytosolic roGFP2-Orp1 redox sensors in Col-0
906 and *jar1-11* leaf cells upon treatment with 10 mM MeV and/or 1 mM JA. Ratios were calculated
907 from the fluorescence values recorded at 535 nm after excitation at 405 nm and 488 nm. Mean
908 ratios \pm SE of different time-points represent data from three replicates, each including three
909 individual seedlings.

910

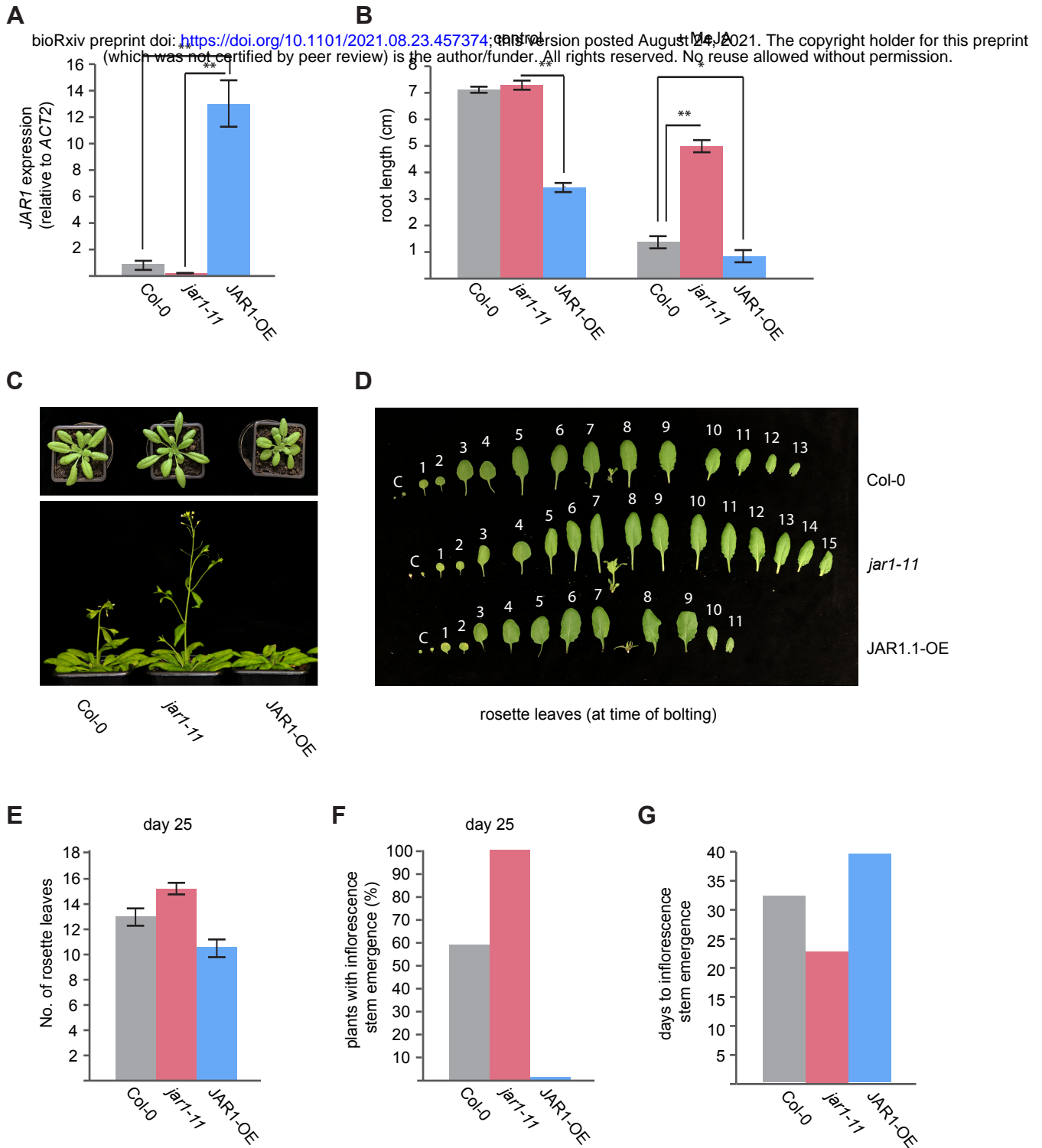


Figure 1. Alteration in *JAR1* expression affects Arabidopsis leaf growth and flowering time.

(A) *JAR1* transcript levels, relative to *ACT2*, in Col-0, *jar1-11* and JAR1-OE determined by RT-qPCR using rosette leaves of 25 days old plants grown on soil. Data were analyzed by one-way ANOVA (** $P < 0.01$) followed by multiple comparison analysis (Tukey HSD test). Data represent means \pm SE from three biological replicates ($n = 3$).

(B) Root length of Col-0, *jar1-11* and JAR1-OE plants grown on 1/2 MS medium with or without 50 μ M MeJA (see also Supplemental Figure S2). Data were analyzed by one-way ANOVA (* $P < 0.05$, ** $P < 0.01$) followed by multiple comparison analysis (Tukey HSD test). Data represent means \pm SE from three biological replicates ($n = 3$), each containing >10 seedlings.

(C) Growth phenotype of Col-0, *jar1-11* and JAR1-OE plants grown on soil under long day conditions after 25 days (upper panel) and 32 days (lower panel).

(D) Detached rosette leaves at the time of inflorescence stem emergence (~ 1 cm stem length) of plants grown on soil in long-day conditions. Leaves were detached at day 32 (Col-0), 25 (*jar1-11*) and day 40 (JAR1-OE).

(E) Rosette leaf numbers at day 25. Data represent means \pm SE from five biological replicates ($n = 5$), each containing a minimum of five individual plants.

(F) Percentage of plants with emerged inflorescence stem of at least 1 cm at day 25.

(G) Average day by which inflorescence stems had emerged. Data represent means from five biological replicates ($n = 5$), each containing a minimum of five individual plants.

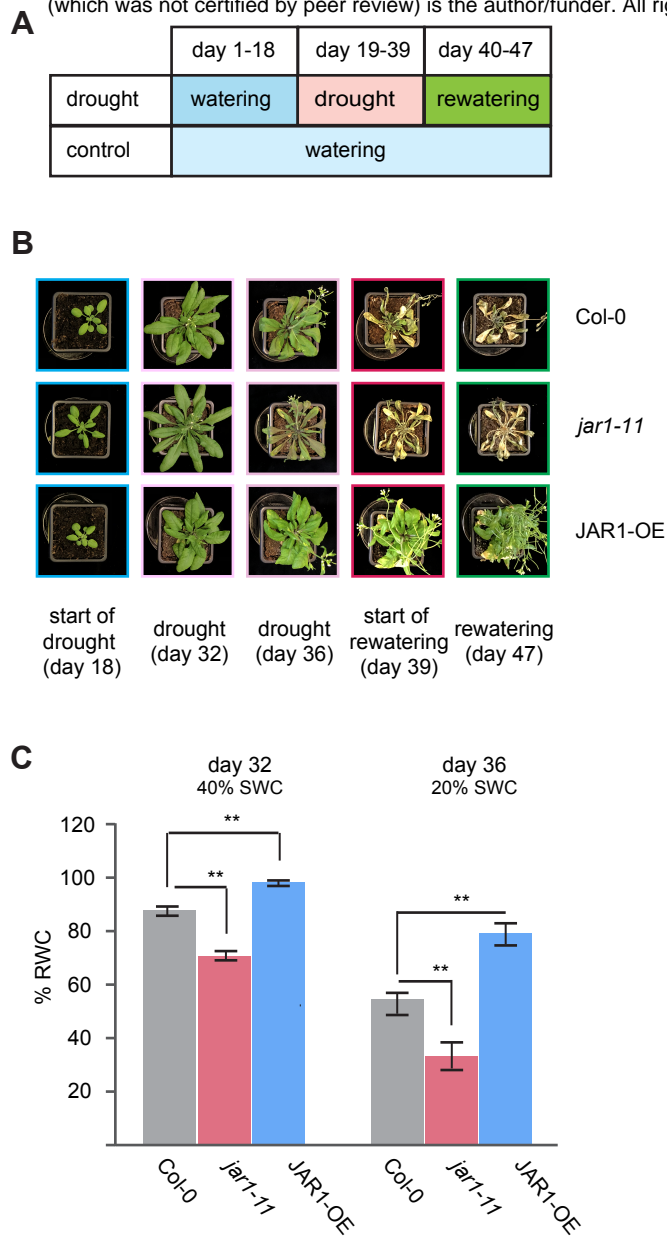


Figure 2. Increased *JAR1* expression positively affects drought stress tolerance.

(A) Schematic representation of the progressive drought stress experiment. Watering was stopped on day 18. Plants were watered again at day 39 when soil water content (SWC) of Col-0 plants reached 10%.

(B) Representative photographs showing plant phenotypes throughout the progressive drought stress experiment (see also Supplemental Figure S4A).

(C) Leaf relative water content (% RWC) of drought-treated plants on day 32 (40 % SWC) and day 36 (20 % SWC). Data represent means \pm SE from five biological replicates (n=5), each containing five individual plants. Data were analyzed by one-way ANOVA (**P<0.01) followed by multiple comparison analysis (Tukey HSD test).

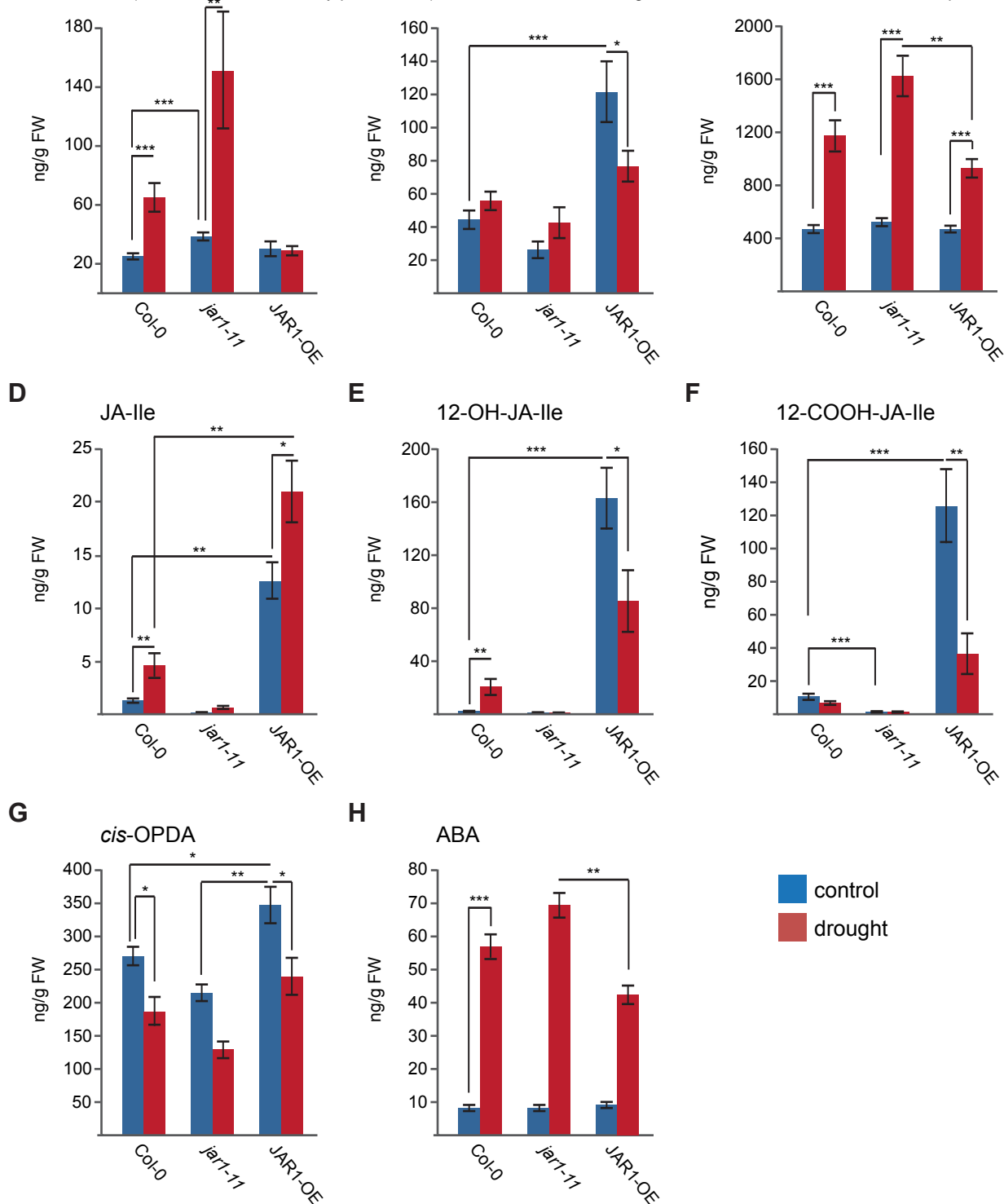


Figure 3. JAR1-dependent changes in the contents of jasmonates and ABA.

The contents of different jasmonates (**A-G**) and ABA (**H**) were determined in rosette leaves of 32-day old plants from wild type (Col-0), *Jar1-11* and JAR1-OE grown under control and drought stress conditions. Compounds measured were jasmonic acid (JA), 12-hydroxy-jasmonic acid (12-OH-JA), 12-hydroxyl-jasmonoyl-glucoside (12-O-Glc-JA), jasmonyl-isoleucine (JA-Ile), 12-hydroxy-jasmonyl-isoleucine (12-OH-JA-Ile), 12-carboxy-jasmonyl-isoleucine (12-COOH-JA-Ile), 12-oxo-phytodienoic acid (*cis*-OPDA), and abscisic acid (ABA). Data represent means \pm SE from six replicates (n=6), each containing pooled extracts from three plants. Data were analyzed by two-way ANOVA (* $P < 0.05$, ** $P < 0.01$, *** $P < 0.001$) followed by multiple comparison analysis (Tukey HSD test).

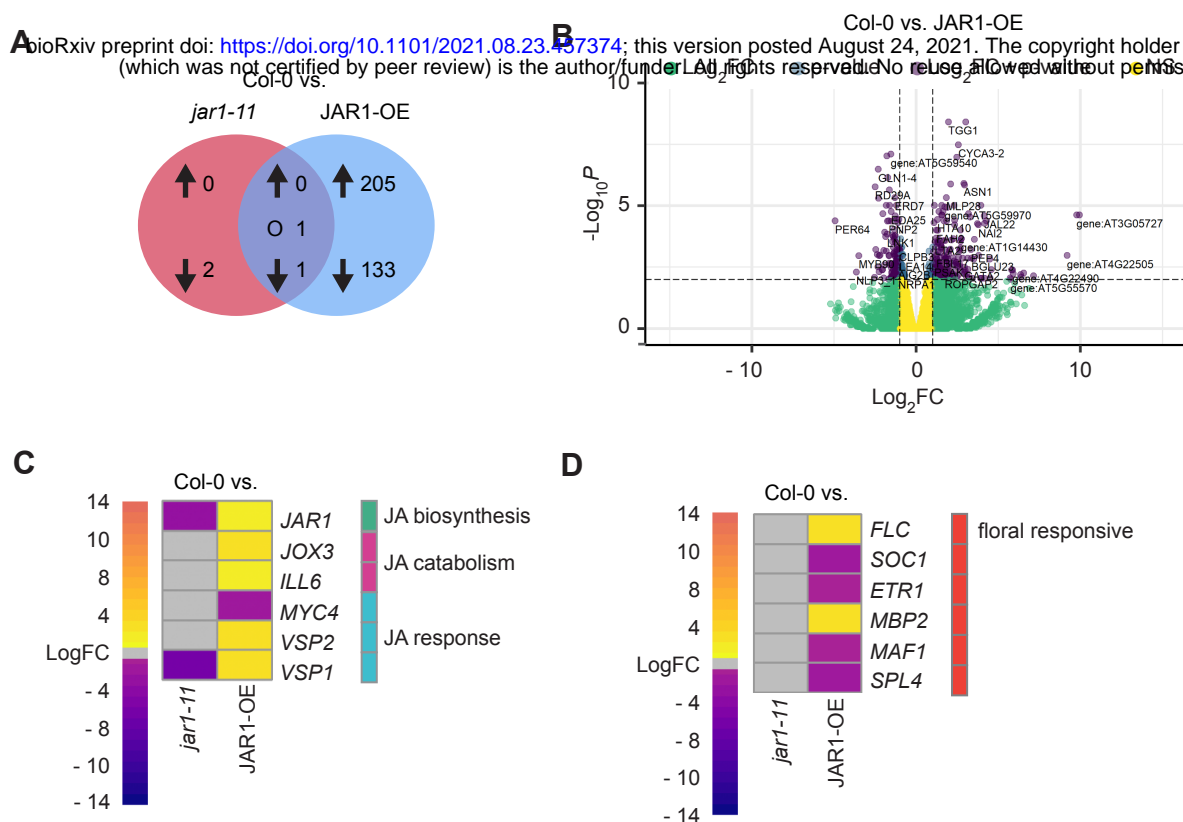


Figure 4. JAR1-dependent changes in gene expression in rosette leaves under normal growth conditions.

(A) Venn diagram showing DEGs (DESeq, adjusted to FDR < 0.01 and LogFC \geq 1) in *jar1-11* and JAR1-OE compared to Col-0 in 32-day old plants under normal growth conditions. Arrows indicate up- and downregulation. "O" indicates counter-regulated genes.

(B) Volcano plot showing statistical significance ($\log_{10}P$) versus magnitude of change (LogFC) of DEGs between Col-0 and JAR1-OE. Violet dots indicate genes that fit the DESeq criteria of FDR < 0.01 and LogFC \geq 1, while green and blue dots represent DEGs that fit only LogFC or FDR, respectively.

(C) and **(D)** Heat maps of genes involved in JA biosynthesis, catabolism and signaling response **(C)** or flowering responsive genes **(D)**. Expression was compared between Col-0 and *jar1-11* or JAR1-OE. Data were analysed using a cut-off of FDR < 0.05 and LogFC \geq 0.5.

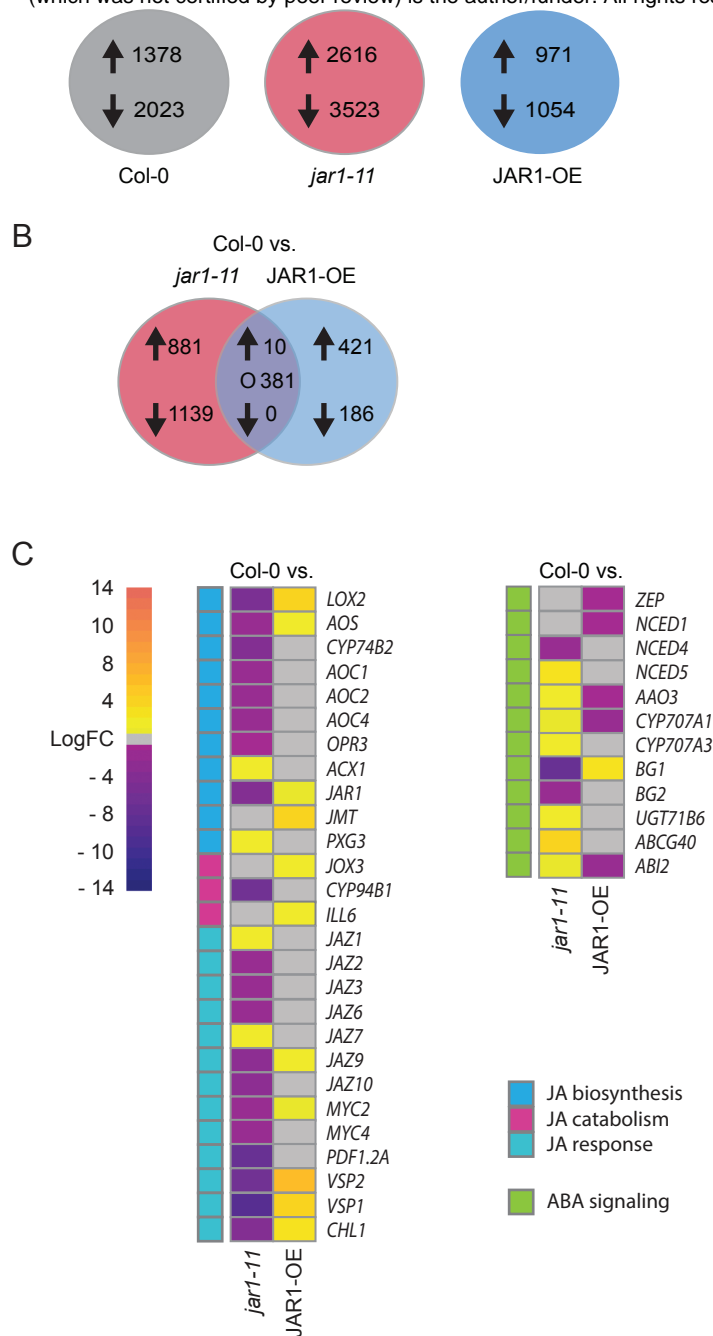


Fig. 5. JAR1-dependent changes in gene expression in rosette leaves under progressive drought.

(A) Number of DEGs (DESeq, adjusted $P < 0.01$ and $\text{LogFC} \geq 1$) between control and drought conditions in Col-0, *jar1-11* and JAR1-OE. Arrows indicate up- and downregulation.

(B) Venn diagram of DEGs (DESeq, adjusted $P < 0.01$ and $\text{LogFC} \geq 1$) in *jar1-11* and JAR1-OE compared to Col-0 under drought conditions. Arrows indicate up- and downregulation. "O" indicates counter-regulated genes.

(C) Heat maps of genes involved in JA biosynthesis, catabolism and signaling response (left) as well as ABA biosynthesis, catabolism and signaling response (right) compared between Col-0 and either *jar1-11* or JAR1-OE, all under drought conditions. Data were analysed using a cut off of $\text{FDR} < 0.05$ and $\text{LogFC} \geq 0.5$.

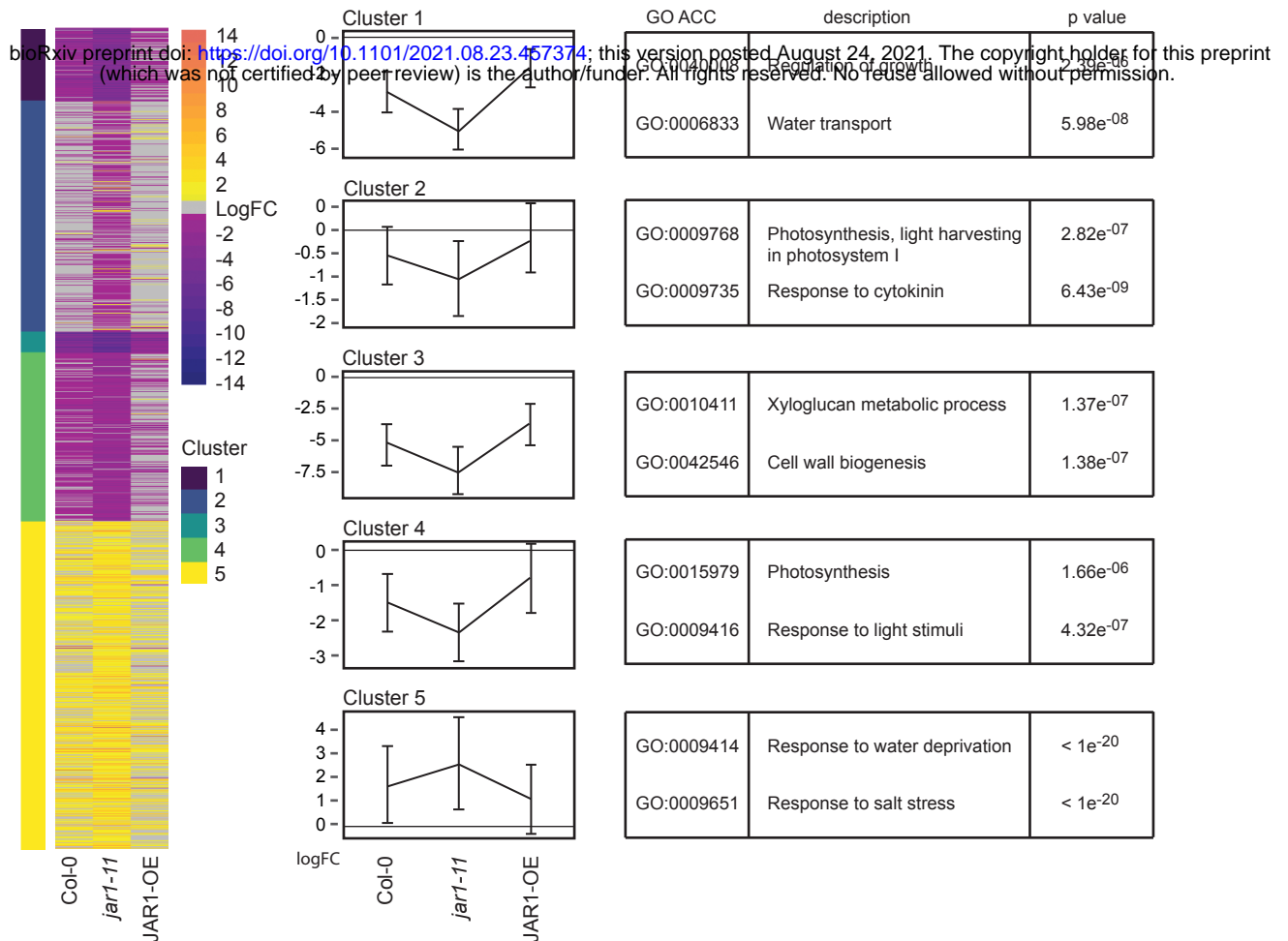


Figure 6. JAR1-dependent transcriptomic variations between drought stress and control conditions.

Heat map (left) and K-means clustering (middle) of genes up- or downregulated under drought compared to control condition in the different plant genotypes. K-means clustering analysis was performed to produce the clusters (DESeq, adjusted FDR < 0.01 and LogFC ≥ 1) and the thin lines represent the mean expression profiles for each cluster (middle). Only genes that are differentially expressed in at least one of the comparisons were used for the cluster analysis. The top two GO terms for each cluster with p values are listed (right).

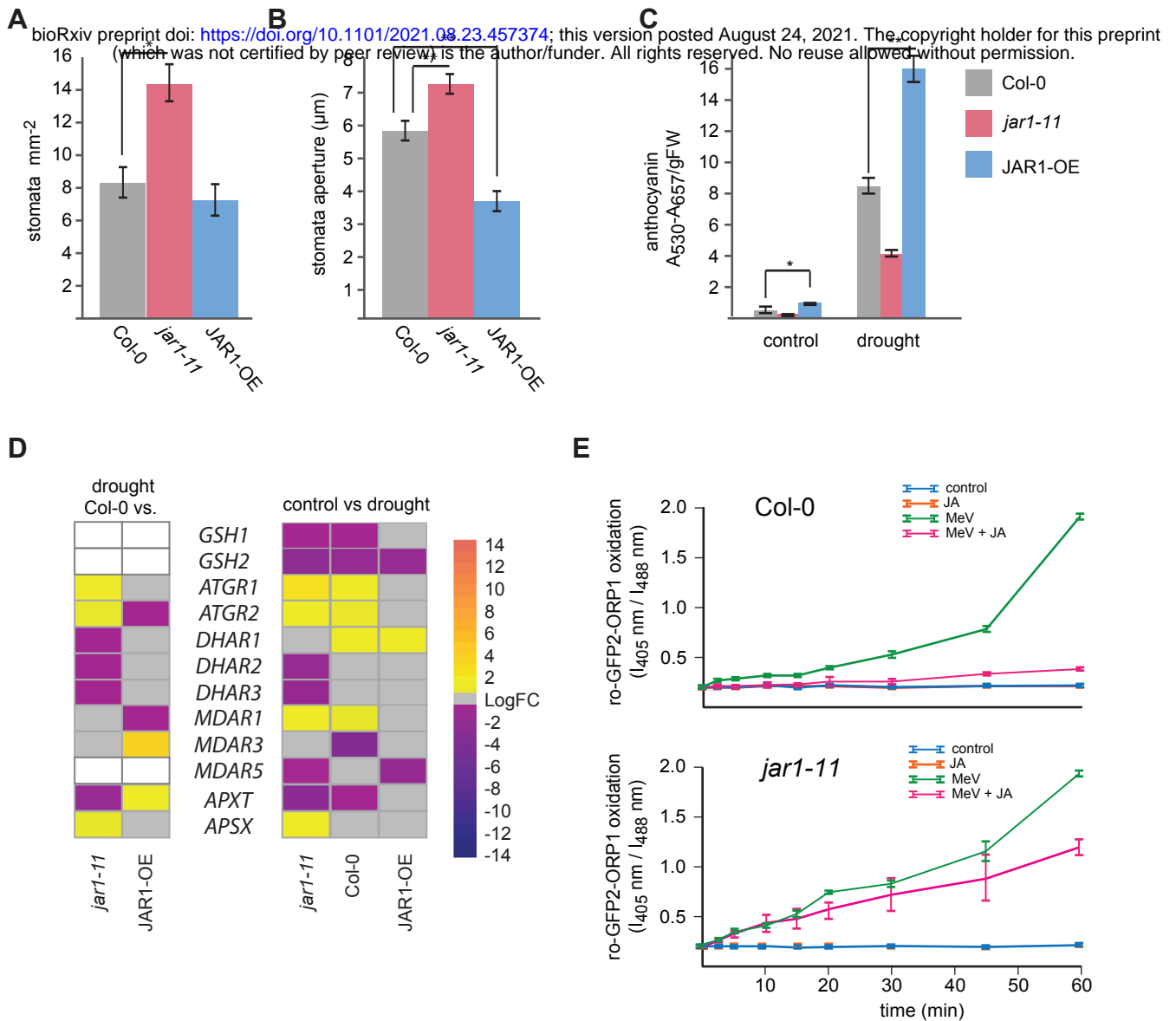


Fig. 7. Effect of JA-Ile on stomatal regulation, anthocyanin content and MV-induced changes in redox status.

(A) and **(B)** Number of stomata **(A)** and stomatal aperture **(B)** measured on leaf No. 6 of plants grown under control conditions at day 21. Data represent means \pm SE from three biological replicates ($n = 3$). For stomatal numbers, each replicate quantified leaves from 5-6 individual plants. For stomatal aperture, each replicate quantified 90 to 100 stomata in leaves from 6-10 individual plants. Data were analyzed by one-way ANOVA ($*P < 0.05$, $**P < 0.01$) followed by multiple comparisons (Tukey HSD test).

(C) Anthocyanin content of different plant genotypes determined in rosette leaves of 32-day old plants grown under control and drought stress conditions. Data represent means \pm SE from 3 replicates ($n=3$), each containing three pooled individual plants. Data were analyzed by one-way ANOVA ($*P < 0.05$, $**P < 0.01$) followed by multiple comparisons (Tukey HSD test).

(D) Heat maps of DEGs involved in the ascorbate-glutathione cycle in *jar1-11* and JAR1-OE compared to Col-0 under drought conditions (left) or between control and drought conditions in Col-0, *jar1-11* and JAR1-OE (right). Data were analysed using a cut-off of $\text{FDR} < 0.05$ and $\text{LogFC} > 0.5$. White boxes indicate genes whose changes did not meet the cut-off criteria.

(E) Real-time monitoring of redox status using cytosolic roGFP2-Orp1 redox sensors in Col-0 and *jar1-11* leaf cells upon treatment with 10 mM MeV and/or 1 mM JA. Ratios were calculated from the fluorescence values recorded at 535 nm after excitation at 405 nm and 488 nm. Mean ratios \pm SE of different time-points represent data from three replicates each including three individual seedlings.

Parsed Citations

- Akter, N., Okuma, E., Sobahan, M. A., Uraji, M., Munemasa, S., Nakamura, Y., Mori, I. C., & Murata, Y. (2013). Negative regulation of methyl jasmonate-induced stomatal closure by glutathione in *Arabidopsis*. *Journal of Plant Growth Regulation*, 32 (1), 208–215. <https://doi.org/10.1007/s00344-012-9291-7>
Google Scholar: [Author Only](#) [Title Only](#) [Author and Title](#)
- Alexa, A., & Rahnenfuhrer, J. (2020). topGO: Enrichment analysis for gene ontology. *R Package Version*, 2 (42), 1-26. <https://doi.org/10.18129/B9.bioc.topGO>
Google Scholar: [Author Only](#) [Title Only](#) [Author and Title](#)
- Armezzani, A., Abad, U., Ali, O., Robin, A. A., Vachez, L., Larrieu, A., Mellerowicz, E. J., Taconnat, L., Battu, V., Stanislas, T., Liu, M., Vernoux, T., Traas, J., & Sassi, M. (2018). Transcriptional induction of cell wall remodelling genes is coupled to microtubule-driven growth isotropy at the shoot apex in *Arabidopsis*. *Development (Cambridge)*, 145 (11), 1-11. <https://doi.org/10.1242/dev.162255>
Google Scholar: [Author Only](#) [Title Only](#) [Author and Title](#)
- Balfagón, D., Sengupta, S., Gómez-Cadenas, A., Fritschi, F. B., Azad, R. K., Mittler, R., & Zandalinasc, S. I. (2019). Jasmonic acid is required for plant acclimation to a combination of high light and heat stress. *Plant Physiology*, 181 (4), 1668–1682. <https://doi.org/10.1104/pp.19.00956>
Google Scholar: [Author Only](#) [Title Only](#) [Author and Title](#)
- Barrs, H., & Weatherley, P. (1962). A re-examination of the relative turgidity technique for estimating water deficits in leaves. *Australian Journal of Biological Sciences*, 15 (3), 413–428. <https://doi.org/10.1071/bi9620413>
Google Scholar: [Author Only](#) [Title Only](#) [Author and Title](#)
- Bell, E., Creelman, R. A., & Mullet, J. E. (1995). A chloroplast lipoxygenase is required for wound-induced jasmonic acid accumulation in *Arabidopsis*. *Proceedings of the National Academy of Sciences U.S.A.*, 92 (19), 8675–8679. <https://doi.org/10.1073/pnas.92.19.8675>
Google Scholar: [Author Only](#) [Title Only](#) [Author and Title](#)
- Benjamini, Y., & Hochberg, Y. (1995). Controlling the false discovery rate: a practical and powerful approach to multiple testing. *Journal of the Royal Statistical Society*, 57 (1), 289–300. <https://www.jstor.org/stable/2346101>
Google Scholar: [Author Only](#) [Title Only](#) [Author and Title](#)
- Bernal, A. J., Jensen, J. K., Harholt, J., Sørensen, S., Møller, I., Blaukopf, C., Johansen, B., De Lotto, R., Pauly, M., Scheller, H. V., & Willats, W. G. T. (2007). Disruption of ATCSLD5 results in reduced growth, reduced xylan and homogalacturonan synthase activity and altered xylan occurrence in *Arabidopsis*. *Plant Journal*, 52 (5), 791–802. <https://doi.org/10.1111/j.1365-3113X.2007.03281.x>
Google Scholar: [Author Only](#) [Title Only](#) [Author and Title](#)
- Bhosale, R., Jewell, J. B., Hollunder, J., Koo, A. J. K., Vuylsteke, M., Michoel, T., Hilson, P., Goossens, A., Howe, G. A., Browse, J., & Maere, S. (2013). Predicting gene function from uncontrolled expression variation among individual wild-type *Arabidopsis* plants. *Plant Cell*, 25 (8), 2865–2877. <https://doi.org/10.1105/tpc.113.112268>
Google Scholar: [Author Only](#) [Title Only](#) [Author and Title](#)
- Capella, A., Menossi, M., Arruda, P., & Benedetti, C. (2001). COI1 affects myrosinase activity and controls the expression of two flower-specific myrosinase-binding protein homologues in *Arabidopsis*. *Planta*, 213 (5), 691–699. <https://doi.org/10.1007/s004250100548>
Google Scholar: [Author Only](#) [Title Only](#) [Author and Title](#)
- Chae, K., Gonong, B. J., Kim, S. C., Kieslich, C. A., Morikis, D., Balasubramanian, S., & Lord, E. M. (2010). A multifaceted study of stigma/style cysteine-rich adhesin (SCA)-like *Arabidopsis* lipid transfer proteins (LTPs) suggests diversified roles for these LTPs in plant growth and reproduction. *Journal of Experimental Botany*, 61 (15), 4277–4290. <https://doi.org/10.1093/jxb/erq228>
Google Scholar: [Author Only](#) [Title Only](#) [Author and Title](#)
- Chambers, J. M., Freeny, A., & Heiberger, R. M. (1992). Analysis of variance; designed experiments. In: Chambers JM, Hastie TJ, eds. *Statistical Models in S*. Chapter 5. Boca Raton, FL: Chapman & Hall/ CRC.
Google Scholar: [Author Only](#) [Title Only](#) [Author and Title](#)
- Cheng, C. Y., Krishnakumar, V., Chan, A. P., Thibaud-Nissen, F., Schobel, S., & Town, C. D. (2017). Araport11: a complete reannotation of the *Arabidopsis thaliana* reference genome. *Plant Journal*, 89 (4), 789–804. <https://doi.org/10.1111/tpj.13415>
Google Scholar: [Author Only](#) [Title Only](#) [Author and Title](#)
- Chini, A., Fonseca, S., Fernández, G., Adie, B., Chico, J. M., Lorenzo, O., García-Casado, G., López-Vidriero, I., Lozano, F. M., Ponce, M. R., Micol, J. L., & Solano, R. (2007). The JAZ family of repressors is the missing link in jasmonate signaling. *Nature*, 448 (7154), 666–671. <https://doi.org/10.1038/nature06006>
Google Scholar: [Author Only](#) [Title Only](#) [Author and Title](#)
- Cho, L. H., Yoon, J., & An, G. (2017). The control of flowering time by environmental factors. *Plant Journal*, 90 (4), 708–719. <https://doi.org/10.1111/tpj.13461>
Google Scholar: [Author Only](#) [Title Only](#) [Author and Title](#)
- Claeys, H., & Inzé, D. (2013). The agony of choice: how plants balance growth and survival under water-limiting conditions. *Plant Physiology*, 162(4), 1768–1779. <https://doi.org/10.1104/pp.113.220921>
Google Scholar: [Author Only](#) [Title Only](#) [Author and Title](#)

Clauw, P., Coppens, F., Korte, A., Herman, D., Slabbinck, B., Dhondt, S., Van Daele, T., De Milde, L., Vermeersch, M., Maleux, K., Maere, S., Gonzalez, N., & Inzé, D. (2016). Leaf growth response to mild drought: natural variation in *Arabidopsis* sheds light on trait architecture. *Plant Cell*, 28 (10), 2417–2434. <https://doi.org/10.1105/tpc.16.00483>

Google Scholar: [Author Only Title Only Author and Title](#)

Daszkowska-Golec, A., & Szarejko, I. (2013). Open or close the gate - stomata action under the control of phytohormones in drought stress conditions. *Frontiers in Plant Science*, 4 (MAY), 1-16. <https://doi.org/10.3389/fpls.2013.00138>

Google Scholar: [Author Only Title Only Author and Title](#)

Datla, R. S. S., Hammerlindl, J. K., Panchuk, B., Pelcher, L. E., & Keller, W. (1992). Modified binary plant transformation vectors with the wild-type gene encoding NPTII. *Gene*, 122 (2), 383-384. [https://doi.org/10.1016/0378-1119\(92\)90232-E](https://doi.org/10.1016/0378-1119(92)90232-E)

Google Scholar: [Author Only Title Only Author and Title](#)

de Ollas, C., Arbona, V., & Gómez-Cadenas, A. (2015a). Jasmonic acid interacts with abscisic acid to regulate plant responses to water stress conditions. *Plant Signaling and Behavior*, 10 (12). <https://doi.org/10.1080/15592324.2015.1078953>

Google Scholar: [Author Only Title Only Author and Title](#)

de Ollas, C., Arbona, V., & Gómez-Cadenas, A. (2015b). Jasmonoyl isoleucine accumulation is needed for abscisic acid build-up in roots of *Arabidopsis* under water stress conditions. *Plant, Cell and Environment*, 38 (10), 2157–2170. <https://doi.org/10.1111/pce.12536>

Google Scholar: [Author Only Title Only Author and Title](#)

Devoto, A., & Turner, J. G. (2005). Jasmonate-regulated *Arabidopsis* stress signaling network. *Physiologia Plantarum*, 123(2), 161–172. <https://doi.org/10.1111/j.1399-3054.2004.00418.x>

Google Scholar: [Author Only Title Only Author and Title](#)

Dombrecht, B., Gang, P. X., Sprague, S. J., Kirkegaard, J. A., Ross, J. J., Reid, J. B., Fitt, G. P., Sewelam, N., Schenk, P. M., Manners, J. M., & Kazana, K. (2007). MYC2 differentially modulates diverse jasmonate-dependent functions in *Arabidopsis*. *Plant Cell*, 19 (7), 2225–2245. <https://doi.org/10.1105/tpc.106.048017>

Google Scholar: [Author Only Title Only Author and Title](#)

Durinck, S., Spellman, P. T., Birney, E., & Huber, W. (2009). Mapping identifiers for the integration of genomic datasets with the R/Bioconductor package biomaRt. *Nature Protocols*, 4 (8), 1184–1191. <https://doi.org/10.1038/nprot.2009.97>

Google Scholar: [Author Only Title Only Author and Title](#)

Fernández-Calvo, P., Chini, A., Fernández-Barbero, G., Chico, J. M., Gimenez-Ibanez, S., Geerinck, J., Solano, R. (2011). The *Arabidopsis* bHLH transcription factors MYC3 and MYC4 are targets of JAZ repressors and act additively with MYC2 in the activation of jasmonate responses. *Plant Cell*, 23 (2), 701–715. <https://doi.org/10.1105/tpc.110.080788>

Google Scholar: [Author Only Title Only Author and Title](#)

Fisher, R. A. (1925). *Statistical Methods for Research Workers*. Oliver and Boyd (Edinburgh). ISBN 0-05-002170-2

Google Scholar: [Author Only Title Only Author and Title](#)

Gaudet, P., Livstone, M. S., Lewis, S. E. & Thomas, P. D. (2011). Phylogenetic-based propagation of functional annotations within the Gene Ontology consortium. *Briefings in Bioinformatics*, 12 (5), 449-462. [10.1093/bib/bbr042](https://doi.org/10.1093/bib/bbr042)

Google Scholar: [Author Only Title Only Author and Title](#)

Gu, F., Bringmann, M., Combs, J. R., Yang, J., Bergmann, D. C., & Nielsen, E. (2016). *Arabidopsis* CSLD5 functions in cell plate formation in a cell cycle-dependent manner. *Plant Cell*, 28 (7), 1722–1737. <https://doi.org/10.1105/tpc.16.00203>

Google Scholar: [Author Only Title Only Author and Title](#)

Guo, Q., Yoshida, Y., Major, I. T., Wang, K., Sugimoto, K., Kapali, G., Havko, N. E., Benning, C., & Howe, G. A. (2018). JAZ repressors of metabolic defense promote growth and reproductive fitness in *Arabidopsis*. *Proceedings of the National Academy of Sciences U.S.A*, 115 (45), E10768–E10777. <https://doi.org/10.1073/pnas.1811828115>

Google Scholar: [Author Only Title Only Author and Title](#)

Gupta, A., Rico-Medina, A., & Caño-Delgado, A. I. (2020). The physiology of plant responses to drought. *Science*, 368 (6488), 266-269. <https://doi.org/10.1126/science.aaz7614>

Google Scholar: [Author Only Title Only Author and Title](#)

Guranowski, A., Miersch, O., Staswick, P. E., Suza, W., & Wasternack, C. (2007). Substrate specificity and products of side-reactions catalyzed by jasmonate:amino acid synthetase (JAR1). *FEBS Letters*, 581 (5), 815–820. <https://doi.org/10.1016/j.febslet.2007.01.049>

Google Scholar: [Author Only Title Only Author and Title](#)

Gutierrez, C. (2009). The *Arabidopsis* cell division cycle. In: *The Arabidopsis Book*, 7, American Society of Plant Biologists, e0120. <https://doi.org/10.1199/tab.0120>

Google Scholar: [Author Only Title Only Author and Title](#)

Han, X., Hu, Y., Zhang, G., Jiang, Y., Chen, X., & Yu, D. (2018). Jasmonate negatively regulates stomatal development in *Arabidopsis* cotyledons. *Plant Physiology*, 176 (4), 2871–2885. <https://doi.org/10.1104/pp.17.00444>

Google Scholar: [Author Only Title Only Author and Title](#)

Hartigan, J. A., & Wong, M. A. (1979). Algorithm AS 136: a K-Means clustering algorithm. *Journal of the Royal Statistical Society*, 28 (1), 100–108. <https://doi.org/10.2307/2346830>

Google Scholar: [Author Only](#) [Title Only](#) [Author and Title](#)

Hickman, R., Van Verk, M. C., Van Dijken, A. J. H., Mendes, M. P., Vroegop-Vos, I. A., Caarls, L., Steenbergen, M., Van der Nagel, I., Wesselink, G. J., Jironkin, A., Talbot, A., Rhodes, J., De Vries, M., Schuurink, R. C., Denby, K., Pieterse, C. M. J., & Van Wees, S. C. M. (2017). Architecture and dynamics of the jasmonic acid gene regulatory network. *Plant Cell*, 29 (9), 2086–2105. <https://doi.org/10.1105/tpc.16.00958>

Google Scholar: [Author Only](#) [Title Only](#) [Author and Title](#)

Horiguchi, G., Nakayama, H., Ishikawa, N., Kubo, M., Demura, T., Fukuda, H., & Tsukaya, H. (2011). ANGUSTIFOLIA3 plays roles in adaxial/abaxial patterning and growth in leaf morphogenesis. *Plant and Cell Physiology*, 52 (1), 112–124. <https://doi.org/10.1093/pcp/pcq178>

Google Scholar: [Author Only](#) [Title Only](#) [Author and Title](#)

Hossain, M. A., Munemasa, S., Uraji, M., Nakamura, Y., Mori, I. C., & Murata, Y. (2011). Involvement of endogenous abscisic acid in methyl jasmonate-induced stomatal closure in *Arabidopsis*. *Plant Physiology*, 156 (1), 430–438. <https://doi.org/10.1104/pp.111.172254>

Google Scholar: [Author Only](#) [Title Only](#) [Author and Title](#)

Howe, G. A., Major, I. T., & Koo, A. J. (2018). Modularity in jasmonate signaling for multistress resilience. *Annual Review of Plant Biology*, 69, 387–415. <https://doi.org/10.1146/annurev-arplant-042817-040047>

Google Scholar: [Author Only](#) [Title Only](#) [Author and Title](#)

Huang, D., Wu, W., Abrams, S. R., & Cutler, A. J. (2008). The relationship of drought-related gene expression in *Arabidopsis thaliana* to hormonal and environmental factors. *Journal of Experimental Botany*, 59 (11), 2991–3007. <https://doi.org/10.1093/jxb/ern155>

Google Scholar: [Author Only](#) [Title Only](#) [Author and Title](#)

Islam, M. M., Tani, C., Watanabe-Sugimoto, M., Uraji, M., Jahan, M. S., Masuda, C., Nakamura, Y., Mori, I. C., & Murata, Y. (2009). Myrosinases, TGG1 and TGG2, redundantly function in ABA and MeJA signaling in *Arabidopsis* guard cells. *Plant and Cell Physiology*, 50 (6), 1171–1175. <https://doi.org/10.1093/pcp/pcp066>

Google Scholar: [Author Only](#) [Title Only](#) [Author and Title](#)

Jimenez-Aleman, G. H., Almeida-Trapp, M., Fernández-Barbero, G., Gimenez-Ibanez, S., Reichelt, M., Vadassery, J., Mithöfer, A., Caballero, J., Boland, W., & Solano, R. (2019). Omega hydroxylated JA-Ile is an endogenous bioactive jasmonate that signals through the canonical jasmonate signaling pathway. *Biochimica et Biophysica Acta - Molecular and Cell Biology of Lipids*, 1864 (12). <https://doi.org/10.1016/j.bbalip.2019.158520>

Google Scholar: [Author Only](#) [Title Only](#) [Author and Title](#)

Katsir, L., Schillmiller, A. L., Staswick, P. E., Sheng, Y. H., & Howe, G. A. (2008). COI1 is a critical component of a receptor for jasmonate and the bacterial virulence factor coronatine. *Proceedings of the National Academy of Sciences of the United States of America*, 105 (19), 7100–7105. <https://doi.org/10.1073/pnas.0802332105>

Google Scholar: [Author Only](#) [Title Only](#) [Author and Title](#)

Kazan, K., & Manners, J. M. (2013). MYC2: The master in action. *Molecular Plant*, 6 (3), 686–703. <https://doi.org/10.1093/mp/sss128>

Google Scholar: [Author Only](#) [Title Only](#) [Author and Title](#)

Kim, J. H., & Kende, H. (2004). A transcriptional coactivator, AtGIF1, is involved in regulating leaf growth and morphology in *Arabidopsis*. *Proceedings of the National Academy of Sciences of the United States of America*, 101 (36), 13374–13379. <https://doi.org/10.1073/pnas.0405450101>

Google Scholar: [Author Only](#) [Title Only](#) [Author and Title](#)

Koo, A. J. (2018). Metabolism of the plant hormone jasmonate: a sentinel for tissue damage and master regulator of stress response. *Phytochemistry Reviews*, 17 (1), 51–80. <https://doi.org/10.1007/s1101-017-9510-8>

Google Scholar: [Author Only](#) [Title Only](#) [Author and Title](#)

Kwak, J. M., Nguyen, V., & Schroeder, J. I. (2006). The role of reactive oxygen species in hormonal responses. *Plant Physiology*, 141 (2), 323–329. <https://doi.org/10.1104/pp.106.079004>

Google Scholar: [Author Only](#) [Title Only](#) [Author and Title](#)

Lee, B. H., Ko, J. H., Lee, S., Lee, Y., Pak, J. H., & Kim, J. H. (2009). The *Arabidopsis* GRF-Interacting Factor gene family performs an overlapping function in determining organ size as well as multiple. *Plant Physiology*, 151 (2), 655–668. <https://doi.org/10.1104/pp.109.141838>

Google Scholar: [Author Only](#) [Title Only](#) [Author and Title](#)

Liu, X., Yue, Y., Li, B., Nie, Y., Li, W., Wu, W. H., & Ma, L. (2007). A G protein-coupled receptor is a plasma membrane receptor for the plant hormone abscisic acid. *Science*, 315 (5819), 1712–1716. <https://doi.org/10.1126/science.1135882>

Google Scholar: [Author Only](#) [Title Only](#) [Author and Title](#)

Liu, N., Staswick, P. E., & Avramova, Z. (2016). Memory responses of jasmonic acid-associated *Arabidopsis* genes to a repeated dehydration stress. *Plant Cell and Environment*, 39 (11), 2515–2529. <https://doi.org/10.1111/pce.12806>

Google Scholar: [Author Only](#) [Title Only](#) [Author and Title](#)

Liu, Z., Li, N., Zhang, Y., & Li, Y. (2020). Transcriptional repression of GIF1 by the KIX-PPD-MYC repressor complex controls seed size in *Arabidopsis*. *Nature Communications*, 11 (1). <https://doi.org/10.1038/s41467-020-15603-3>

Google Scholar: [Author Only](#) [Title Only](#) [Author and Title](#)

Lorenzo, O., Chico, J. M., Sánchez-Serrano, J. J., & Solano, R. (2004). JASMONATE-INSENSITIVE1 encodes a MYC transcription factor essential to discriminate between different jasmonate-regulated defense responses in arabidopsis. *Plant Cell*, 16 (7), 1938–1950.

<https://doi.org/10.1105/tpc.022319>

Google Scholar: [Author Only Title Only Author and Title](#)

Merlot, S., Gosti, F., Guerrier, D., Vavasseur, A., & Giraudat, J. (2001). The ABI1 and ABI2 protein phosphatases 2C act in a negative feedback regulatory loop of the abscisic acid signaling pathway. *Plant Journal*, 25(3). <https://doi.org/10.1046/j.1365-313X.2001.00965.x>

Google Scholar: [Author Only Title Only Author and Title](#)

Meyer, A J., Brach, T., Marty, L., Kreye, S., Rouhier, N., Jacquot, J. P., & Hell, R. (2007). Redox-sensitive GFP in *Arabidopsis thaliana* is a quantitative biosensor for the redox potential of the cellular glutathione redox buffer. *Plant Journal*, 52 (5), 973–986.

<https://doi.org/10.1111/j.1365-313X.2007.03280.x>

Google Scholar: [Author Only Title Only Author and Title](#)

Michaels, S. D., & Amasino, R. M. (2001). Loss of FLOWERING LOCUS C activity eliminates the late-flowering phenotype of FRIGADA and autonomous pathway mutations but not responsiveness to vernalization. *Plant Cell*, 13(4), 935-941.

<https://doi.org/10.1105/tpc.13.4.935>

Google Scholar: [Author Only Title Only Author and Title](#)

Mouradov, A., Cremer, F., & Coupland, G. (2002). Control of flowering time: interacting pathways as a basis for diversity. *Plant Cell*, 14 (SUPPL.), S111-S130. <https://doi.org/10.1105/tpc.001362>

Google Scholar: [Author Only Title Only Author and Title](#)

Miersch, O., Neumerkel, J., Dippe, M., Stenzel, I., & Wasternack, C. (2008). Hydroxylated jasmonates are commonly occurring metabolites of jasmonic acid and contribute to a partial switch-off in jasmonate signaling. *New Phytologist*, 177 (1), 114–127.

<https://doi.org/10.1111/j.1469-8137.2007.02252.x>

Google Scholar: [Author Only Title Only Author and Title](#)

Mizuno, T. & Yamashino, T. (2008). Comparative transcriptome of diurnally oscillating genes and hormone-responsive genes in *Arabidopsis thaliana*: insight into circadian clock-controlled daily responses to common ambient stresses in plants. *Plant Cell and Physiology*, 49 (3): 481–487. [10.1093/pcp/pcn008](https://doi.org/10.1093/pcp/pcn008)

Google Scholar: [Author Only Title Only Author and Title](#)

Neff, M. M., & Chory, J. (1998). Genetic interactions between phytochrome A, phytochrome B, and cryptochrome 1 during arabidopsis development. *Plant Physiology*, 118 (1), 27–36. <https://doi.org/10.1104/pp.118.1.27>

Google Scholar: [Author Only Title Only Author and Title](#)

Nietzel, T., Elsässer, M., Ruberti, C., Steinbeck, J., Ugalde, J. M., Fuchs, P., Wagner, S., Ostermann, L., Moseler, A., Lemke, P., Fricker, M. D., Müller-Schüssele, S. J., Moerschbacher, B. M., Costa, A., Meyer, A J., & Schwarzländer, M. (2019). The fluorescent protein sensor roGFP2-Orp1 monitors in vivo H₂O₂ and thiol redox integration and elucidates intracellular H₂O₂ dynamics during elicitor-induced oxidative burst in *Arabidopsis*. *New Phytologist*, 221 (3), 1649–1664. <https://doi.org/10.1111/nph.15550>

Google Scholar: [Author Only Title Only Author and Title](#)

Noctor, G., Mhamdi, A., & Foyer, C. H. (2014). The roles of reactive oxygen metabolism in drought: Not so cut and dried. *Plant Physiology*, 164 (4), 1636–1648. <https://doi.org/10.1104/pp.113.233478>

Google Scholar: [Author Only Title Only Author and Title](#)

Noir, S., Bömer, M., Takahashi, N., Ishida, T., Tsui, T. L., Balbi, V., Shanahan, H., Sugimoto, K., & Devoto, A. (2013). Jasmonate controls leaf growth by repressing cell proliferation and the onset of endoreduplication while maintaining a potential stand-by mode. *Plant Physiology*, 161 (4), 1930–1951. <https://doi.org/10.1104/pp.113.214908>

Google Scholar: [Author Only Title Only Author and Title](#)

Poudel, A. N., Holtsclaw, R. E., Kimberlin, A., Sen, S., Zeng, S., Joshi, T., Lei, Z., Sumner, L. W., Singh, K., Matsuura, H., & Koo, A. J. (2019). 12-Hydroxy-Jasmonoyl-Isoleucine is an active jasmonate that signals through CORONATINE INSENSITIVE 1 and contributes to the wound response in *Arabidopsis*. *Plant and Cell Physiology*, 60 (10), 2152–2166. <https://doi.org/10.1093/pcp/pcz109>

Google Scholar: [Author Only Title Only Author and Title](#)

R Core Team (2020). R: A language and environment for statistical computing. R Foundation for Statistical Computing, Vienna, Austria. URL <https://www.R-project.org/>.

Google Scholar: [Author Only Title Only Author and Title](#)

Raghavendra, A S., & Reddy, K. B. (1987). Action of proline on stomata differs from that of abscisic acid, g-substances, or methyl jasmonate. *Plant Physiology*, 83(4), 732-734. <https://doi.org/10.1104/pp.83.4.732>

Google Scholar: [Author Only Title Only Author and Title](#)

Ratcliffe, O. J., Nadzan, G. C., Reuber, T. L., & Riechmann, J. L. (2001). Regulation of flowering in *Arabidopsis* by an FLC homologue. *Plant Physiology*, 126(1), 122-132. <https://doi.org/10.1104/pp.126.1.122>

Google Scholar: [Author Only Title Only Author and Title](#)

Rhaman, M. S., Nakamura, T., Nakamura, Y., Munemasa, S., & Murata, Y. (2020). The myrosinases TGG1 and TGG2 function redundantly in reactive carbonyl species signaling in *Arabidopsis* guard cells. *Plant and Cell Physiology*, 61 (5), 967–977.

<https://doi.org/10.1093/pcp/pcaa024>

Google Scholar: [Author Only Title Only Author and Title](#)

Richter, R., Kinoshita, A., Vincent, C., Martinez-Gallegos, R., Gao, H., van Driel, A. D., Hyun, Y., Mateos, J. L., & Coupland, G. (2019). Floral regulators FLC and SOC1 directly regulate expression of the B3-type transcription factor TARGET of FLC and SVP 1 at the Arabidopsis shoot apex via antagonistic chromatin modifications. *PLoS Genetics*, 15 (4), 1-27.

<https://doi.org/10.1371/journal.pgen.1008065>

Google Scholar: [Author Only](#) [Title Only](#) [Author and Title](#)

Robinson, M. D., McCarthy, D. J., & Smyth, G. K. (2009). edgeR: A Bioconductor package for differential expression analysis of digital gene expression data. *Bioinformatics*, 26 (1), 139–140. <https://doi.org/10.1093/bioinformatics/btp616>

Google Scholar: [Author Only](#) [Title Only](#) [Author and Title](#)

Robinson, M. D., & Oshlack, A. (2010). Deseq2论文附录. *Genome Biology*, 11 (3), 1–9. <http://genomebiology.com/2010/11/3/R25>

Google Scholar: [Author Only](#) [Title Only](#) [Author and Title](#)

Sasaki-Sekimoto, Y., Taki, N., Obayashi, T., Aono, M., Matsumoto, F., Sakurai, N., Suzuki, H., Hirai, M. Y., Noji, M., Saito, K., Masuda, T., Takamiya, K. I., Shibata, D., & Ohta, H. (2005). Coordinated activation of metabolic pathways for antioxidants and defence compounds by jasmonates and their roles in stress tolerance in Arabidopsis. *Plant Journal*, 44 (4), 653–668. <https://doi.org/10.1111/j.1365-313X.2005.02560.x>

Google Scholar: [Author Only](#) [Title Only](#) [Author and Title](#)

Savchenko, T. V., Rolletschek, H., & Dehesh, K. (2019). Jasmonates-Mediated rewiring of central metabolism regulates adaptive responses. *Plant and Cell Physiology*, 60 (12), 2613–2620. <https://doi.org/10.1093/pcp/pcz181>

Google Scholar: [Author Only](#) [Title Only](#) [Author and Title](#)

Shan, X., Zhang, Y., Peng, W., Wang, Z., & Xie, D. (2009). Molecular mechanism for jasmonate-induction of anthocyanin accumulation in Arabidopsis. *Journal of Experimental Botany*, 60 (13), 3849–3860. <https://doi.org/10.1093/jxb/erp223>

Google Scholar: [Author Only](#) [Title Only](#) [Author and Title](#)

Schwarzländer, M., Fricker, M. D. & Sweetlove, L. J. (2009). Monitoring the in vivo redox state of plant mitochondria: effect of respiratory inhibitors, abiotic stress and assessment of recovery from oxidative challenge. *Biochimica et Biophysica Acta*, 1787 (5), 468–475. [10.1016/j.bbabi.2009.01.020](https://doi.org/10.1016/j.bbabi.2009.01.020)

Google Scholar: [Author Only](#) [Title Only](#) [Author and Title](#)

Smirnova, E., Marquis, V., Poirier, L., Aubert, Y., Zumsteg, J., Ménard, R., Miesch, L., & Heitz, T. (2017). Jasmonic Acid Oxidase 2 hydroxylates jasmonic acid and represses basal defense and resistance responses against Botrytis cinerea infection. *Molecular Plant*, 10 (9), 1159–1173. <https://doi.org/10.1016/j.molp.2017.07.010>

Google Scholar: [Author Only](#) [Title Only](#) [Author and Title](#)

Staswick, P. E., Su, W., & Howell, S. H. (1992). Methyl jasmonate inhibition of root growth and induction of a leaf protein are decreased in an Arabidopsis thaliana mutant. *Proceedings of the National Academy of Sciences of the United States of America*, 89(15), 6837-6840. <https://doi.org/10.1073/pnas.89.15.6837>

Google Scholar: [Author Only](#) [Title Only](#) [Author and Title](#)

Staswick, P. E., & Tiryaki, I. (2004). The oxylipin signal jasmonic acid is activated by an enzyme that conjugate it to isoleucine in Arabidopsis W inside box sign. *Plant Cell*, 16 (8), 2117–2127. <https://doi.org/10.1105/tpc.104.023549>

Google Scholar: [Author Only](#) [Title Only](#) [Author and Title](#)

Staswick, P. E., Tiryaki, I., & Rowe, M. L. (2002). Jasmonate response locus JAR1 and several related Arabidopsis genes encode enzymes of the firefly luciferase superfamily that show activity on jasmonic, salicylic, and indole-3-acetic acids in an assay for adenylation. *Plant Cell*, 14 (6), 1405–1415. <https://doi.org/10.1105/tpc.000885>

Google Scholar: [Author Only](#) [Title Only](#) [Author and Title](#)

Staswick, P. E., Yuen, G. Y., & Lehman, C. C. (1998). Jasmonate signaling mutants of Arabidopsis are susceptible to the soil fungus Pythium irregulare. *Plant Journal*, 15 (6), 747–754. <https://doi.org/10.1046/j.1365-313X.1998.00265.x>

Google Scholar: [Author Only](#) [Title Only](#) [Author and Title](#)

Suza, W. P., & Staswick, P. E. (2008). The role of JAR1 in jasmonoyl-I-isoleucine production during Arabidopsis wound response. *Planta*, 227 (6), 1221–1232. <https://doi.org/10.1007/s00425-008-0694-4>

Google Scholar: [Author Only](#) [Title Only](#) [Author and Title](#)

Thines, B., Katsir, L., Melotto, M., Niu, Y., Mandaokar, A., Liu, G., Nomura, K., He, S. Y., Howe, G. A., & Browse, J. (2007). JAZ repressor proteins are targets of the SCFCO11 complex during jasmonate signaling. *Nature*, 448 (7154), 661–665. <https://doi.org/10.1038/nature05960>

Google Scholar: [Author Only](#) [Title Only](#) [Author and Title](#)

Thorndike, R. L. (1953). Who belongs in the family? *Psychometrika*, 18 (4), 267–276. <https://doi.org/10.1007/BF02289263>

Google Scholar: [Author Only](#) [Title Only](#) [Author and Title](#)

Tukey, J. W. (1949). Comparing Individual Means in the Analysis of Variance. *International Biometric Society*, 5 (2), 99–114. <https://doi.org/http://www.jstor.org/stable/3001913>

Google Scholar: [Author Only](#) [Title Only](#) [Author and Title](#)

Ullah, C., Tsai, C. J., Unsicker, S. B., Xue, L., Reichelt, M., Gershenzon, J., & Hammerbacher, A. (2019). Salicylic acid activates poplar defense against the biotrophic rust fungus Melampsora larici-populina via increased biosynthesis of catechin and proanthocyanidins.

New Phytologist, 221 (2), 960–975. <https://doi.org/10.1111/nph.15396>

Google Scholar: [Author Only](#) [Title Only](#) [Author and Title](#)

Ulrich, L., Schmitz, J., Thurow, C., & Gatz, C. (2021). The jasmonoyl-isooleucine receptor CORONATINE INSENSITIVE1 suppresses defense gene expression in Arabidopsis roots independently of its ligand. *The Plant Journal*. <https://doi.org/10.1111/tpj.15372>

Google Scholar: [Author Only](#) [Title Only](#) [Author and Title](#)

Vadassery, J., Reichelt, M., Hause, B., Gershenzon, J., Boland, W., & Mithöfer, A. (2012). CML42-mediated calcium signaling coordinates responses to Spodoptera herbivory and abiotic stresses in Arabidopsis. *Plant Physiology*, 159 (3), 1159–1175. <https://doi.org/10.1104/pp.112.198150>

Google Scholar: [Author Only](#) [Title Only](#) [Author and Title](#)

Verma, V., Ravindran, P., & Kumar, P. P. (2016). Plant hormone-mediated regulation of stress responses. *BMC Plant Biology*, 16 (1), 1–10. <https://doi.org/10.1186/s12870-016-0771-y>

Google Scholar: [Author Only](#) [Title Only](#) [Author and Title](#)

Wasternack, C., & Hause, B. (2013). Jasmonates: Biosynthesis, perception, signal transduction and action in plant stress response, growth and development. An update to the 2007 review in *Annals of Botany*. *Annals of Botany*, 111 (6), 1021–1058. <https://doi.org/10.1093/aob/mct067>

Google Scholar: [Author Only](#) [Title Only](#) [Author and Title](#)

Wasternack, Claus. (2017). A plant's balance of growth and defense – revisited. *New Phytologist*, 215 (4), 1291–1294. <https://doi.org/10.1111/nph.14720>

Google Scholar: [Author Only](#) [Title Only](#) [Author and Title](#)

Wasternack, Claus, & Song, S. (2017). Jasmonates: Biosynthesis, metabolism, and signaling by proteins activating and repressing transcription. *Journal of Experimental Botany*, 68 (6), 1303–1321. <https://doi.org/10.1093/jxb/erw443>

Google Scholar: [Author Only](#) [Title Only](#) [Author and Title](#)

Widemann, E., Miesch, L., Lugan, R., Holder, E., Heinrich, C., Aubert, Y., Miesch, M., Pinot, F., & Heitz, T. (2013). The amidohydrolases IAR3 and ILL6 contribute to jasmonoyl-isooleucine hormone turnover and generate 12-hydroxyjasmonic acid upon wounding in arabidopsis leaves. *Journal of Biological Chemistry*, 288 (44), 31701–31714. <https://doi.org/10.1074/jbc.M113.499228>

Google Scholar: [Author Only](#) [Title Only](#) [Author and Title](#)

Wu, G., & Poethig, R. S. (2006). Temporal regulation of shoot development in Arabidopsis thaliana by miRr156 and its target SPL3. *Development*, 133 (18), 3539–3547. <https://doi.org/10.1242/dev.02521>

Google Scholar: [Author Only](#) [Title Only](#) [Author and Title](#)

Xia, X. J., Zhou, Y. H., Shi, K., Zhou, J., Foyer, C. H., & Yu, J. Q. (2015). Interplay between reactive oxygen species and hormones in the control of plant development and stress tolerance. *Journal of Experimental Botany*, 66 (10), 2839–2856. <https://doi.org/10.1093/jxb/erv089>

Google Scholar: [Author Only](#) [Title Only](#) [Author and Title](#)

Xiang, C., & Oliver, D. J. (1998). Glutathione metabolic genes coordinately respond to heavy metals and jasmonic acid in arabidopsis. *Plant Cell*, 10 (9), 1539–1550. <https://doi.org/10.1105/tpc.10.9.1539>

Google Scholar: [Author Only](#) [Title Only](#) [Author and Title](#)

Xie, D., Feys, B. F., James, S., Nieto-rostro, M., & Turner, J. G. (1998). COI1: an Arabidopsis gene required for jasmonate-regulated defense and fertility. *Science*, 280, 1091–1094. [10.1126/science.280.5366.1091](https://doi.org/10.1126/science.280.5366.1091)

Google Scholar: [Author Only](#) [Title Only](#) [Author and Title](#)

Xu, Z. Y., Kim, D. H., & Hwang, I. (2013). ABA homeostasis and signaling involving multiple subcellular compartments and multiple receptors. *Plant Cell Reports*, 32 (6), 807–813. <https://doi.org/10.1007/s00299-013-1396-3>

Google Scholar: [Author Only](#) [Title Only](#) [Author and Title](#)

Yan, J., Zhang, C., Gu, M., Bai, Z., Zhang, W., Qi, T., Cheng, Z., Peng, W., Luo, H., Nan, F., Wang, Z., & Xie, D. (2009). The arabidopsis CORONATINE INSENSITIVE1 protein is a jasmonate receptor. *Plant Cell*, 21 (8), 2220–2236. <https://doi.org/10.1105/tpc.109.065730>

Google Scholar: [Author Only](#) [Title Only](#) [Author and Title](#)

Yang, J., Duan, G., Li, C., Liu, L., Han, G., Zhang, Y., & Wang, C. (2019). The crosstalks between jasmonic acid and other plant hormone signaling highlight the involvement of jasmonic acid as a core component in plant response to biotic and abiotic stresses. *Frontiers in Plant Science*, 10. <https://doi.org/10.3389/fpls.2019.01349>

Google Scholar: [Author Only](#) [Title Only](#) [Author and Title](#)

Yang, S., Vanderbeld, B., Wan, J., & Huang, Y. (2010). Narrowing down the targets: towards successful genetic engineering of drought-tolerant crops. *Molecular Plant*, 3(3), 469–490. Oxford University Press. <https://doi.org/10.1093/mp/ssp016>

Google Scholar: [Author Only](#) [Title Only](#) [Author and Title](#)

Yates, A. D., Achuthan, P., Akanni, W., Allen, J., Allen, J., Alvarez-Jarreta, J., Amode, M. R., Armean, I. M., Azov, A. G., Bennett, R., Bhai, J., Billis, K., Boddu, S., Marugán, J. C., Cummins, C., Davidson, C., Dodiya, K., Fatima, R., Gall, A., ... Flicek, P. (2020). Ensembl 2020. *Nucleic Acids Research*, 48 (D1), D682–D688. <https://doi.org/10.1093/nar/gkz966>

Google Scholar: [Author Only](#) [Title Only](#) [Author and Title](#)

Zander, M., Lewsey, M. G., Clark, N. M., Yin, L., Bartlett, A., Saldierna Guzmán, J. P., Hann, E., Langford, A. E., Jow, B., Wise, A., Nery, J. R., Chen, H., Bar-Joseph, Z., Walley, J. W., Solano, R., & Ecker, J. R. (2020). Integrated multi-omics framework of the plant response to jasmonic acid. *Nature Plants*, 6 (3), 290–302. <https://doi.org/10.1038/s41477-020-0605-7>

Google Scholar: [Author Only](#) [Title Only](#) [Author and Title](#)

Zhai, Q., Zhang, X., Wu, F., Feng, H., Deng, L., Xu, L., Zhang, M., Wang, Q., & Li, C. (2015). Transcriptional mechanism of jasmonate receptor COI1-mediated delay of flowering time in arabidopsis. *Plant Cell*, 27 (10), 2814–2828. <https://doi.org/10.1105/tpc.15.00619>

Google Scholar: [Author Only](#) [Title Only](#) [Author and Title](#)

Zhang, Y., & Turner, J. G. (2008). Wound-induced endogenous jasmonates stunt plant growth by inhibiting mitosis. *PLoS ONE*, 3 (11). <https://doi.org/10.1371/journal.pone.0003699>

Google Scholar: [Author Only](#) [Title Only](#) [Author and Title](#)

Züst, T., & Agrawal, A. A. (2017). Trade-Offs between plant growth and defense against insect herbivory: an emerging mechanistic synthesis. *Annual Review of Plant Biology*, 68, 513–534. <https://doi.org/10.1146/annurev-arplant-042916-040856>

Google Scholar: [Author Only](#) [Title Only](#) [Author and Title](#)